Georgia State University
ScholarWorks @ Georgia State University

Psychology Dissertations   Department of Psychology

5-1-2019

Structural Network Properties and Their Relation to Cognitive Flexibility and Neurological Risk Factors in Adult Survivors of Pediatric Brain Tumors

Sabrina Na

Follow this and additional works at: https://scholarworks.gsu.edu/psych_diss

STRUCTURAL NETWORK PROPERTIES AND THEIR RELATION TO

COGNITIVE FLEXBILITY AND NEUROLOGICAL RISK FACTORS IN ADULT

SURVIVORS OF PEDIATRIC BRAIN TUMORS

by

SABRINA NA

Under the Direction of Tricia Z. King, PhD

ABSTRACT

Neuroimaging techniques have been used to investigate the neurobiological mechanisms of cognitive deficits in survivors of childhood brain tumors. Graph theory is a quantitative method that characterizes brains as a complex system. By modeling brain regions as 'nodes' and white matter tracts between each brain region pair as 'edges,' graph theory provides metrics that quantify the topological properties of networks. Given that brain tumor survivorship is associated with focal and diffuse impairments, a network analysis can provide complementary information to previous neuroimaging studies in this clinical group. This study used diffusion-weighted imaging and deterministic tractography to examine the properties of the structural networks in 38 adult survivors of pediatric brain tumors (Mean age=22.5, 55% female, mean years post diagnosis=14.1 (6.2), Range post diagnosis = 4.5-30 years). Results of this study suggest that long term survivorship is associated with altered structural networks with respect to measures of integration, segregation, and centrality. Further, properties of the network mediate differences in

cognitive flexibility performance between survivors and healthy peers, and mediate the

relationship between cumulative neurological risk and cognitive flexibility performance.

INDEX WORDS: Diffusion-weighted imaging, Deterministic tractography, Graph theory,

Executive functioning, Long-term outcomes, Brain tumor survivorship, Cognitive

flexibility

STRUCTURAL NETWORK PROPERTIES AND THEIR RELATION TO

COGNITIVE FLEXIBILITY AND NEUROLOGICAL RISK FACTORS IN ADULT

SURVIVORS OF PEDIATRIC BRAIN TUMORS

by

SABRINA NA

A Dissertation Submitted in Partial Fulfillment of the Requirements for the Degree of

Doctor of Philosophy

in the College of Arts and Sciences

Georgia State University

2019

STRUCTURAL NETWORK PROPERTIES AND THEIR RELATION TO

COGNITIVE FLEXIBILITY AND NEUROLOGICAL RISK FACTORS IN ADULT

SURVIVORS OF PEDIATRIC BRAIN TUMORS

by

SABRINA NA

Committee Chair: Tricia Z. King

Committee: Bruce Crosson

Vonetta Dotson

Longchuan Li

Electronic Version Approved:

Office of Graduate Studies

College of Arts and Sciences

Georgia State University

May 2019

DEDICATION

I would like to dedicate this work to my parents, Jung and Sangsin. They gave everything they had to give me the best education they could, and I am deeply grateful for their years of love, patience and unimaginable sacrifice. Thank you for refraining from asking me how long it would take for me to finish my degree! I am so proud to be your daughter. I would also like to dedicate this dissertation to my wonderful partner, Wesley, who has supported me through graduate school and forced me to go outside precisely when I needed fresh air. And to my pups, Emma and Brinkley, who are all the self-care that anyone could ever need.

ACKNOWLEDGEMENTS

Firstly, I would like to express my deepest appreciation to my committee chair and academic advisor, Dr. Tricia King. I would also like to acknowledge Dr. Longchuan Li, who was so willing to meet with me and answer every graph theory question that I had. I am deeply grateful for his expertise. I am also deeply grateful for Dr. Crosson's and Dr. Dotson's assistance. I am grateful to the individuals and families who participated in this study and generously contributed their time and effort. I would also like to acknowledge the members of the Developmental Neuropsychology Across the Lifespan (DNP-ATL) Laboratory research team for their help with data acquisition and management.

TABLE OF CONTENTS

LIST OF TABLES

LIST OF FIGURES

1   INTRODUCTION

1.1   Brain Tumor Survivorship

Cancers of the brain and central nervous system are the second most prevalent type of cancers in children. In the United States alone, an estimated 4820 children will be diagnosed with a brain tumor in 2017 (Ostrom et al., 2016). Medical and technological advances in cancer treatments have resulted in improved survival rates for children with brain tumors (Porter, McCarthy, Freels, Kim, & Davis, 2010). For instance, 5 year survival rates for medulloblastoma, which is the most common malignant brain tumor in children, have risen from 29% to 70% over the past several decades (Smoll, 2012). Research has shifted to emphasize the quality of survival as increasing numbers of these survivors reach adulthood. Hence, a body of research has emerged to identify psychosocial and neurobiological factors that predict poor outcomes, identify protective factors that promote resilience, and develop effective treatments and interventions to address the problems that arise in survivors as they age (Lassaletta, Bouffet, Mabbott, & Kulkarni, 2015; Mulhern, Merchant, Gajjar, Reddick, & Kun, 2004; Murdaugh, King, & O'Toole, 2017).

Research on long-term outcomes of adult survivors of pediatric brain tumors has demonstrated late effects even decades after initial diagnosis and treatment. Several studies of large cohorts of adult survivors have utilized self- and proxy-reports to investigate health-related quality of life (HRQOL). Survivors who are at least five years post diagnosis and their caregivers frequently report significant physical, social, emotional and cognitive effects due to brain tumor and associated treatments (Barakat et al., 2015; Crom et al., 2014). Furthermore, a longitudinal study of the same cohort of adult survivors over the course of a decade indicated progressive

declines in HRQOL, suggesting that survivors experience increased difficulties as they age (Duckworth et al., 2015).

There are substantial physical late effects that are common in pediatric brain tumor survivors. These include higher incidence of cardiovascular risk factors, endocrine complications (e.g., reduced growth, hypothyroidism, pubertal disorders, gonadal dysfunction), sensory changes such as decreased vision and hearing, fatigue, as well as higher risk of developing new cancers (Bereket, 2015; Ehrstedt et al., 2016; Felicetti et al., 2015; Geenen et al., 2007; Gunnes et al., 2016; Hummel et al., 2015; Inskip et al., 2016; Turner, Rey-Casserly, Liptak, & Chordas, 2009). Pain is also a common complaint in this group, with an increase in prevalence and severity noted across a sample of survivors in a 10 year longitudinal study (Nayiager et al., 2015).

Research also suggests that adult survivors of pediatric brain tumors face significant functional limitations. Survivors use more special education services in school, have lower educational attainment, lower rates of school graduation and lower levels of employment relative to the overall population and other cancer survivors that do not involve the central nervous system (Edelstein et al., 2011; Ellenberg et al., 2009; Kelaghan et al., 1988; Robison et al., 2005; Seaver et al., 1994; Ullrich & Embry, 2012).

Survivors who are more than five years past their diagnosis also report more subjective changes in cognition when compared to their healthy siblings, as well as other childhood cancer survivors (Crom et al., 2014; McClellan et al., 2013; Nayiager et al., 2015). A qualitative study examining the narratives surrounding physical, emotional, cognitive, and social quality of life in adolescent and young adult survivors at least 5 years post diagnosis suggested that cognitive

limitations were the most salient for them amidst all domains of functioning (Hobbie et al., 2016).

Early performance studies of cognitive functioning in survivors were completed using broad intellectual functioning measures. Survivors have lower full scale intelligence quotients (IQ) than their healthy peers (Gragert & Ris, 2011), and, moreover, exhibit declines in their full scale IQ by a mean level of 2.55 points every year past their age at diagnosis (Palmer et al., 2001; Spiegler, Bouffet, 2004). This continued decline is attributed to the inability of adult survivors to acquire new skills and information at a rate comparable to their healthy same-age peers, rather than a loss of previously acquired information (Palmer et al., 2001; Saury & Emanuelson, 2011). A meta-analysis of 29 studies comparing IQs in pediatric brain tumor survivors to age-matched controls or population based norms found large effect sizes for full scale IQ score differences (d=-0.79, large effect), with a larger effect on perceptual-based reasoning skills (d=-.90, large effect) when compared to verbal-based reasoning skills (d=-.54, medium effect) (de Ruiter, van Mourik, Schouten-van Meeteren, Grootenhuis, & Oosterlaan, 2013). It should be acknowledged that some research studies, primarily in samples investigating survivors of low-risk brain tumors, do not show significant differences in average IQ between survivors and healthy controls; however, when evaluating the percentage of survivors who meet cutoff scores for clinical impairment, these studies generally find that survivors fall into the clinically impaired range at higher rates compared to controls (Turner et al., 2009).

Although these early studies have established the existence of significant differences in distal outcomes (i.e., academic achievement, vocational achievement, broad IQ) between adult survivors of pediatric brain tumors and their same-aged peers, global measures lack the sensitivity to identify specific neurocognitive domains that are impacted in survivors. Thus,

recent research studies have utilized more comprehensive neuropsychological batteries to investigate specific neurocognitive domains that underlie the gap in functional outcomes between survivors and healthy same-aged peers.

A quantitative review of 39 studies that examined neurocognitive domains in child brain tumor survivors who were 11 years old on average, and an average of 4.2 years posttreatment, found significant effects to global cognitive domains (i.e., global IQ, verbal IQ, nonverbal IQ), academic domains (i.e., spelling, math, reading), and specific neurocognitive domains (i.e., attention, verbal memory, visual-spatial skill, psychomotor skill, and language) as a result of brain tumor diagnosis and treatment (Robinson et al., 2010). There was a large mean effect size when averaging across all domains (Hedge's g = -0.91).

Another quantitative review of 38 studies examining neurocognitive domains in survivors of brain tumors of the posterior fossa suggested that there were diffuse effects to cognitive functioning even though tumors were constrained to the posterior fossa (Robinson, Fraley, Pearson, Kuttesch, & Compas, 2013). The participants in these studies were also primarily children or young adults (mean age = 11.6 years) and were on average 4 years posttreatment. The study found large effect sizes for the domains of attention, executive functions, psychomotor skill, processing speed, verbal memory and visual-spatial skill. Medium effect sizes were present for the domains of language and visual memory. Survivor performance on many domains were at least 1 standard deviation below their same-age peers. The study also found that age at diagnosis and radiation therapy were significant moderators; individuals who were younger when they were diagnosed or had radiation therapy treatment had worse cognitive outcomes.

A qualitative review of studies examining more long-term outcomes in adult survivors of pediatric brain tumors also suggested diffuse effects to neurocognitive functioning. The authors

also noted that there is no specific profile associated with brain tumor survivors. However, there appeared to be higher risks to the domains of attention, working memory, processing speed, new learning, visuospatial skills, visuomotor skills and executive functioning as a result of brain tumors and treatments (Gragert & Ris, 2011). A recently empirically tested model suggested that deficits in attention, working memory, and processing speed skills contribute negatively to intellectual and academic long term outcomes in adult survivors of pediatric brain tumors (King, Ailion, Fox, & Hufstetler, 2017).

It is important to note that there is large variability in the outcomes of survivors, which warrants investigation into the factors that predict those who are at risk for poor outcomes. Prior research has converged on demographic factors (gender, age at diagnosis, years since diagnosis), brain tumor factors (tumor type, tumor location, presence of hydrocephalus, presence of seizures), and treatment factors (presence and dosage of radiation, chemotherapeutic agents) that vary between patients and contribute differentially to outcomes (de Ruiter et al., 2013; Edelstein et al., 2011; Gragert & Ris, 2011; Ris & Noll, 1994).

1.2   Neurotoxic Effects of Brain Tumor and Treatments in Survivors

It is difficult to parse apart the individual contributions of each risk factor because survivors receive a combination of treatments and vary with respect to demographic factors as well as brain tumor type and location. Neurobiological research investigating the mechanisms of each treatment type has shed light on how these risk factors contribute to changes in the brain and ultimately affect functional outcomes. Neuroimaging techniques, which provide *in vivo* brain structure and function information, have been invaluable in helping test the theories regarding mechanisms of treatment-induced brain injury. For instance, diffusion-weighted imaging measures the rate and direction of water diffusion. These measurements have been used as

indirect metrics to describe microstructural properties of various brain structures, including white matter tracts. Further, tractography methods are used to reconstruct 3D maps of white matter pathways in the brain based on mathematical algorithms. Methods like these can quantify changes occurring at the microstructural level and describe the types of changes that occur to the brain due to brain tumors and associated treatments.

The presence and dosage of radiation is widely considered to have the most detrimental impact on outcomes in survivors (Saury & Emanuelson, 2011). Radiation therapy is used to treat malignant brain tumors to halt cancer growth and promote tumor cell death (Lin, Jackson, & Vujaskovic, 2016). However, as radiation therapy does not discriminate between healthy and cancerous cells, radiation therapy can result in diffuse negative effects to functioning. A meta-analysis evaluating the cognitive sequelae in adults diagnosed and treated with medulloblastomas as children concluded that survivors treated with radiotherapy had lower IQ scores than brain tumor survivors who were treated with other types of treatments (de Ruiter et al., 2013). In addition, higher dosages of radiation were associated with poorer performance in many neurocognitive domains, lower health-related quality of life, and more adverse physical, cognitive and emotional effects (Gragert & Ris, 2011; van Dijk et al., 2013).

Contemporary models for radiation-induced brain injury contend that there are dynamic interactions that occur among many different types of cells that result in acute, early delayed, and late delayed brain injury (Greene-Schloesser et al., 2012). Neuroradiological imaging in clinical settings have observed transient demyelination within the first six months after radiation, which typically resolve on their own. The late delayed phase of radiation, however, is associated with irreversible progression of vascular abnormalities, demyelination and necrosis (Zhang, Yang, & Tian, 2015). The causes of these changes are likely multifactorial and include damage to

endothelial cells, loss of oligodendrocyte type-2 astrocytes, sustained microglial activation and astrocytic proliferation which contribute to a chronic inflammatory state and oxidative stress to the brain, and changes in neuronal synaptic efficiency, cellular activity, and gene expression (Greene-Schloesser, Moore, & Robbins, 2013).

A longitudinal study used diffusion-weighted imaging techniques to examine effects of radiation dosage to white matter in adults with high grade gliomas over the course of one year (Connor et al., 2016). The study found a linear relationship between the dosage of radiation and levels of white matter damage. Further, longer periods of time since treatment resulted in progressive white matter damage, which was thought to be due to progressive demyelination. This progression of white matter damage is consistent with findings from longitudinal cognitive studies of adult survivors who have received radiation treatment. Specifically, worse outcomes were associated with a longer time since radiation therapy, with continued declines in IQ, executive functions, attention and working memory many years post diagnosis and treatment (Briere, Scott, McNall-Knapp, & Adams, 2008; Edelstein et al., 2011; Spiegler, Bouffet, Greenberg, Rutka, & Mabbott, 2004).

Other modes of treatments are associated with increased risk for poorer outcomes. Although chemotherapy is widely accepted to be less neurotoxic than radiation, it nevertheless has subtle effects on cognitive outcomes (Moleski, 2000). A review of adult survivors of various types of pediatric cancers treated with chemotherapy (but not radiation) concluded that the domains of attention, executive functioning, visual processing, and visual-motor skills were negatively affected years after treatment (Anderson & Kunin-Batson, 2009). Hypothesized biomolecular mechanisms also suggest multi-factorial causes including increased inflammatory response in the brain, higher oxidative stress, and less effective neuronal repair (Ahles & Saykin,

2007; Moleski, 2000). Neuroimaging studies have found reduced volumes of white matter, gray matter, and the hippocampus, as well as cortical atrophy, leukoencephalopathy and microangiopathy as a result of chemotherapy treatment (Ren, St Clair, & Butterfield, 2017).

Hydrocephalus is also a common neurological condition that occurs in brain tumor survivors. The brain tumor obstructs the flow of cerebrospinal fluid, causing fluid buildup in the ventricles of the brain. This results in increased intraventricular pressure, lower perfusion and edema of periventricular tissue and subsequent damage to periventricular white matter (Krishnamurthy & Li, 2014). When compared to adult survivors without shunts (a device used to treat hydrocephalus by relieving pressure from fluid buildup), survivors with shunts had lower IQs and achievement scores, as well as greater impairments in visual-motor functioning (Hardy, Bonner, Willard, Watral, & Gururangan, 2008).

Lastly, the presence of the tumor and subsequent resection via neurosurgery also have long-term effects. Studies of low-risk brain tumor survivors who were only treated with surgery suggest that there is a high level of variability in adaptive skills and outcomes, and that these survivors are at risk for subtle long-term cognitive effects (Ris & Beebe, 2008). Resection of the brain tumor results in a loss of brain tissue and possible axonal degeneration in areas of the brain that are in the same neural pathway but distal to the site of the lesion. Several clinical studies have used tractography in adult patients to model changes that occur to white matter pathways due to the brain tumor. Slow-growing tumors which do not infiltrate into nearby healthy tissue resulted in displacement of white matter tracts, while fast-growing tumors resulted in displacement, infiltration and disruption of white matter tracts (Nilsson, Rutka, Snead, Raybaud, & Widjaja, 2008; Wei, Guo, & Mikulis, 2014). Studies employing a longitudinal approach have shown that white matter tracts returned to normal position and normal anatomy following

resection, and that this return to normal position correlated with improvement in motor functioning. However, there were also persistent effects after surgery, including thinning, interruptions, and reductions in tract size (Lazar, Alexander, Thottakara, Badie, & Field, 2005).

It is important to note that many studies lack the power to examine these risk factors individually in their studies with multivariate modeling approaches due to limited sample sizes and heterogeneity in their sample. As such, several studies have employed the Neurological Predictor Scale, a measure that incorporates type of tumor treatments and other neurological risk factors into on cumulative score, to examine how the cumulative nature of these risk factors affect outcomes (Micklewright, King, Morris, & Krawiecki, 2008). Research suggests that higher neurological and treatment risk is associated with poorer intelligence and adaptive functioning child survivors of pediatric brain tumor (McCurdy, Rane, Daly, & Jacobson, 2016; Micklewright et al., 2008; Papazoglou, King, Morris, & Krawiecki, 2008). Further, this measure is significantly correlated with intelligence, adaptive functioning, processing speed, working memory and attention outcomes over and above each individual risk factor in adult survivors of pediatric brain tumors (King & Na, 2016; Taiwo, Na, & King, 2017).

1.3 Structural Neuroimaging Studies in Brain Tumor Survivors

Neuroimaging studies conducted in brain tumor survivors have indicated that changes occur on macrostructural and microstructural levels of the brain. Anatomical changes, such as cortical and cerebellar atrophy and leukoencephalopathy can occur as late effects of brain tumors (Riva et al., 2002). However, research has suggested that these visible anatomic changes correlate poorly with measures of behavior and function (Rueckriegel et al., 2010). As such, quantifiable metrics of macrostructural and microstructural properties are commonly used to investigate brain-behavior relationships.

On the macrostructural level, studies have found that total brain volumes and overall white matter volumes are significantly lower in survivors compared to age-matched controls (Jayakar, King, Morris, & Na, 2015; Reddick et al., 2005; Riggs et al., 2014). With respect to gray matter, a study of long-term adult survivors of low-grade cerebellar tumor in childhood suggested atypical grey matter development; results showed increased grey matter density in the bilateral cingulum, left orbitofrontal cortex and left hippocampus. In survivors, higher density in these regions was correlated with decreased processing speed and executive functioning. Secondary analyses suggested that hydrocephalus may account for some of these brain changes, as ventricle volume correlated significantly with gray matter density (Moberget et al., 2015).

Given recent literature regarding the hippocampus as a site of adult neurogenesis and synaptic plasticity, several studies have conducted investigations on hippocampal volume in survivors of pediatric brain tumor. Studies of both child and adult survivors of brain tumors indicate reduced volumes of subcortical structures such as the hippocampus and putamen (Jayakar et al., 2015; Riggs et al., 2014). These studies also reported that hippocampal volumes are associated with memory performance. A longitudinal study investigating child survivors of medulloblastoma up to 5 years post radiation and chemotherapy found progressive decreases in left and right hippocampal volume for two to three years post treatment before returning to normal growth patterns (Nagel et al., 2004).

Overall, neuroimaging studies evaluating macrostructural properties of the brain and hippocampal volumes suggest reduced whole brain volumes, reduced white matter volumes, increased gray matter densities, and reduced hippocampal volumes. Moreover, these findings extend to more than a decade past initial diagnosis and highlight long-lasting effects of neurotoxic treatments such as radiation.

Neuroimaging studies in survivors have also evaluated the microstructural properties of white matter by using diffusion-weighted imaging. As mentioned previously, this method provides an index of white matter integrity; it is hypothesized that brain tumor and adjuvant treatments such as radiation result in demyelination and therefore lower white matter integrity in survivors. Studies have found that average white matter integrity in the brain is reduced in child survivors and long-term adult survivors compared to controls (Aukema et al., 2009; Mabbott, Noseworthy, Bouffet, Laughlin, & Rockel, 2006; Moberget et al., 2015; Reddick et al., 2014). Moreover, the level of changes in overall white matter integrity is significantly correlated with broad intellectual outcomes in child survivors of brain tumor (Khong et al., 2006; Mabbott, Noseworthy, Bouffet, Rockel, & Laughlin, 2006; Rueckriegel, Bruhn, Thomale, & Hernaiz Driever, 2015), as well as adult survivors of brain tumor more than a decade postdiagnosis (King, Wang, & Mao, 2015).

Studies using diffusion-weighted imaging have also identified specific regions and tracts that are affected in the brain. One of the earliest neuroimaging studies of child medulloblastoma survivors treated with radiation found significant and diffuse white matter reductions in the cerebellar hemispheres, pons, medulla oblongata, frontal and parietal periventricular white matter, and corona radiata. Moreover, the authors found that despite there being higher levels of radiation in the posterior fossa, there was significantly more reduction in supratentorial white matter compared to the posterior fossa; the authors posited that supratentorial white matter may be more susceptible to radiation damage (Khong et al., 2003). Accordingly, a follow-up study of child medulloblastoma survivors further tested whether the frontal lobe was more susceptible than other supratentorial regions (i.e., parietal lobe). The authors found that there were more reductions in white matter integrity of the frontal lobe compared to the parietal lobe even though

both regions received same the same radiation dosage, and suggested that frontal regions are more vulnerable in brain tumor survivors (Qiu, Kwong, Chan, Leung, & Khong, 2007). Alternatively, it is possible that their findings were reflective of motion artifacts rather than differences in susceptibility to radiation; due to the biomechanics of the human neck, the frontal lobe is more susceptible to motion compared to the parietal or occipital lobes. Higher levels of motion in the frontal lobe could account for larger levels of differences. This potential confound, however, was not addressed in these research studies.

Studies of child survivors of pediatric brain tumors also have found lower white matter integrity in specific tracts compared to healthy controls. Tracts that have been commonly implicated in these studies include the corpus callosum, anterior and posterior limbs of the internal capsule, inferior frontal white matter, high frontal white matter, inferior fronto-occipital fasciculus and uncinate fasciculus (Aukema et al., 2009; Mabbott, Noseworthy, Bouffet, Rockel, et al., 2006; Palmer et al., 2012; Riggs et al., 2014; Rueckriegel et al., 2010).

Moreover, the integrity and volume of specific tracts is associated with performance on neurocognitive measures in child survivors of brain tumors. For instance, the integrity of the splenium, as well as the white matter integrity of the entire corpus callosum was correlated positively with processing speed measures, while the integrity of the right inferior fronto-occipital fasciculus was correlated with motor speed measures (Aukema et al., 2009). Regions in the corpus callosum, post-thalamic radiation and external callosum differentially related to processing speed measures in survivors versus age, sex and race matched controls (Palmer et al., 2012). Frontocerebellar tract volumes were correlated with full scale IQ and measures of fine motor dysfunction in adolescent medulloblastoma and juvenile pilocytic astrocytoma survivors (Rueckriegel et al., 2015). Poorer white matter integrity of the cerebello-thalamo-cerebral tract

was associated with poorer performance on working memory measures (Law et al., 2011). The level of damage to the uncinate fasciculus was correlated with a general memory index in children (Riggs et al., 2014).

Several studies have also collected data on very long term outcomes of adult survivors of childhood brain tumors to investigate the continued effects of survivorship. An exploratory study of 20 survivors of medulloblastoma who were on average 29 years old at evaluation and 18 years postdiagnosis examined whether white matter integrity in the left and right frontal, parietal, and temporal regions were related to performance measures of executive function (Brinkman et al., 2012). The study found that fractional anisotropy in the parietal lobe was positively associated with working memory, radial diffusivity in both parietal lobes was negatively correlated with shifting attention, radial diffusivity in the temporal lobe was negatively correlated with shifting attention and cognitive flexibility, and fractional anisotropy in the temporal lobes was associated with measures of cognitive fluency. However, this study had several limitations. For instance, the authors did not correct for multiple comparisons even though they conducted correlations on all of their measures of white matter integrity in multiple regions of the brain with all of their neurocognitive measures. Second, they did not employ a control group; as such, the study could not conclude whether there were reductions in white matter integrity in their survivor sample. Further, given the large regions of interest that were employed, there was little specificity to their findings.

Two other studies have evaluated microstructural properties of white matter in very long-term survivors of pediatric brain tumors compared to a healthy control group. These studies extended the neuroimaging findings of childhood brain tumor studies to suggest that reductions in white matter integrity persist in survivors who are at least one decade past their diagnosis and

treatment. A study of 27 adult pediatric brain tumor survivors who were an average of 22.7 years

old when evaluated and 13.7 years postdiagnosis found diffuse regions where the relationships

between broad intellectual functioning and white matter integrity were significantly different

between survivors and healthy same-age peers. These regions included the corpus callosum,

bilateral frontal medial regions, frontal pole, middle temporal, left superior frontal, right inferior

frontal, right frontal orbital regions (King, Wang, et al., 2015).

Another study of an overlapping sample of adult pediatric brain tumor survivors found

reductions in the white matter integrity of the arcuate fasciculus compared to controls. The study

also found that the white matter integrity of the parietotemporal-occipitotemporal and the inferior

fronto-ocicipital fasciculus tract tracts correlated with measures of word reading in survivors.

Further, the study showed that the relationship between white matter integrity of these two tracts

and measures of word reading were mediated by processing speed in survivors (Smith, King,

Jayakar, & Morris, 2014).

Notably, the same risk factors identified in neuropsychological studies that are associated

with poorer functional outcomes also are related to lower overall white matter integrity and

lower white matter integrity in specific tracts. These risk factors include younger age at

treatment, longer time since treatment and higher radiation treatment intensity (King, Wang, et

al., 2015; Law et al., 2011; Reddick et al., 2014). Despite the preponderance of findings suggest

the neurotoxic effects of radiation, it should be noted that several studies have established white

matter disruptions in survivors with low-risk brain tumors who only underwent tumor resection.

These studies found that survivors with low-risk tumors and few neurological risk factors still

share similar distributions of effects to white matter tracts but with a lower level of change when

compared to survivors who underwent more significant neurotoxic treatments (King, Wang, et al., 2015; Rueckriegel et al., 2010).

Taken together, these structural neuroimaging studies have provided valuable insights onto the effects that occur in the brain due to a brain tumor, adjuvant treatments, and other neurological risk factors. Overall, there are global effects to the brain with respect to overall brain volumes and white matter volumes; survivors exhibit lower volumes compared to healthy controls. There is also evidence of effects to specific areas and tracts. Furthermore, these changes in neurobiology correlate with broad measures of intellectual functioning as well as specific neurocognitive domains such as processing speed, working memory, memory, word reading, and executive functioning.

1.4   Network Approaches to Understanding the Brain

Structural neuroimaging studies in survivors of brain tumors so far primarily have used a univariate framework to identify specific regions of the brain that differ between survivors and age-matched controls, based on the assumption that discrete regions of the brain are responsible for specific functions. However, newer emerging frameworks emphasize connectivity between brain regions as a way of investigating how distal brain regions work together as a concerted system. This new framework, called graph theory (or network analysis), marries two different perspectives: segregation (i.e., local regions are responsible for certain functions) and integration (i.e., the brain works as a system). Specific regions of the brain are considered to have localized functions, but graph theory approaches emphasize how each brain region is connected to other brain regions in a system (Rubinov & Sporns, 2010). Graph theory approaches can answer questions about how ensembles of brain regions work together in a unified network. This systems level approach can provide complementary information to traditional neuroimaging

techniques especially when examining higher-order behaviors that depend on the integration of information from spatially distributed regions in the brain (Figure 1). Given the relatively new contributions of this literature, a short primer is provided.
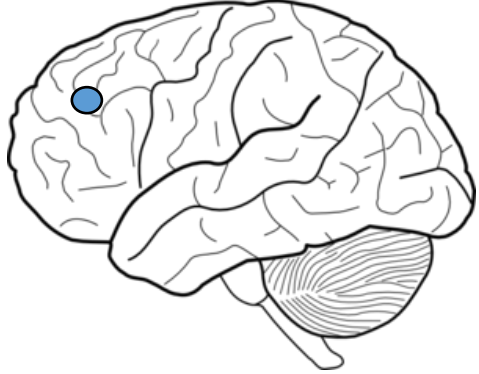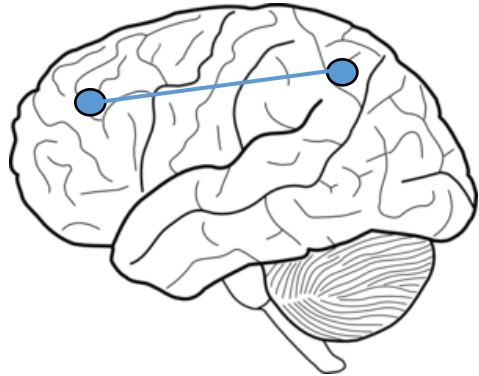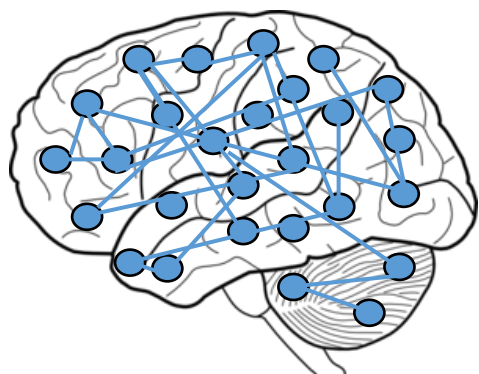
	Description	
Univariate	In univariate approaches, the researcher measures a certain brain property (e.g., average level of functional activation over time, magnitude of white matter integrity) in discrete regions of interest. Measurements from each of these brain regions are typically averaged and compared to another group with t-tests.	
Bivariate	Bivariate approaches are used to measure the extent to which the measurement (e.g., electrical signal over time) from one region of interest is related to the measurement from a second region. These approaches include Pearson correlations and partial correlations to calculate connectivity.	
Multivariate	In multivariate approaches, many regions of the brain (defined as nodes) are selected and analyzed at once. The connectivity between all region pairs (defined as edges) are calculated to yield a complex network. Graph analysis is used to provide quantitative measurements of local and global properties of the overall network.	

Figure 1. Statistical approaches to understanding brain structure and function

Graph analysis methodology has been developed within the last decade to describe the large-scale macroscopic relationships that arise as a result of complex interactions of brain regions (Sporns, 2012). Graph theory is a branch of mathematics that provides quantitative

metrics to describe properties of complex graphs. When applied to the brain, graph analysis

methodology provides metrics to describe properties of 1) brain regions, 2) the connections

between each brain region pair, and 3) the emergent properties of all of these interactions

together in a network. Thus, graph theory is a method used to describe local and global network

properties of the brain and is particularly apt when studying clinical populations where

impairments result from diffuse injury (He & Evans, 2010). Studies utilizing graph analysis for

various neurological disorders including multiple sclerosis, epilepsy, stroke, and Alzheimer's

Disease (AD) have shown that the clinical presentation and the magnitude of impairment is

related to the integrity of these brain networks (Bullmore & Sporns, 2009).

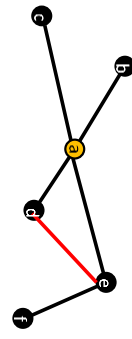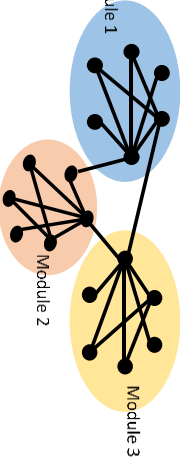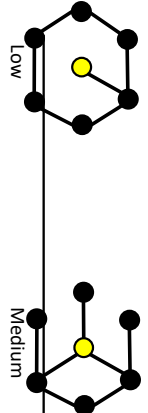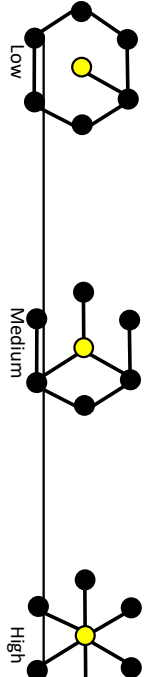| Category	Metric	Definition	Example	Interpretation Within Neuroimaging Context
Basic components	Node	Regions	Nodes are represented by black dots in the diagram to the right	Nodes are defined by the researcher.
	Edge	Relationships between nodes	Edges are represented by the black lines connecting node pairs	Edges are defined by the researcher.
	Density	Proportion of existing edges in the network out of the total possible edges	There are 15 potential edges in a network made of 6 nodes. The network on the right has 6 existing edges. The density of the network is 6/15 = 0.4	Density is a property of the network
Measures of segregation	Clustering coefficient, C	The probability that the neighbors of the node are also connected to each other in the form of a triangle	Clustering coefficient of node a = 1/6. Node a's neighbors are b, c, d, and e. Only 1 node pair (e-d) is connected and form a triangle with node a (marked in red). 6 total node connections are possible with node a's neighbors (b-c, c-d, e-d, b-e, c-e, b-d).	A network with a high clustering coefficient is thought to represent a network with high level of processing that is completed locally within small region.
	Modularity, Q	Existence of communities that have more connections with one another than expected in a random null model	 Module 1, Module 2, Module 3	High modularity is thought to suggest the existence of many modules (communities of nodes) with specialized functions.
Measures of integration	Path Length, L	The fewest # of edges between two nodes	Path length from node b to f = 3 (marked in red). Characteristic path length is equal to the average of all the distances between each node and all other nodes.	Low characteristic path length is thought to relate to high levels of global processing (i.e., information is processed through spatially distributed regions across the brain)
	Global Efficiency, E_{glob}	Inverse of path length, L	Efficiency from node b to f= Inverse of 3= 1/3	High global efficiency suggests high capacity for parallel processing, and high levels of global processing.
Measures of centrality	Betweenness Centrality, B*,	# of shortest paths that must pass through the node	 Low, Medium, High	High betweenness centrality suggests a node that is important for processing in that network, and has a large influence on the transfer of information throughout the network
	Hub disruption index	Summary measure describing the preferential impact to hubs.	If the hub disruption index is calculated from the betweenness centrality values, a plot is created where the x axis represents the average betweenness centrality for each node in the healthy control group, and the y axis represents the difference between the betweenness centrality for each node between the patient vs. the average healthy group. The slope of the best-fit line through this data is the hub disruption index.	A high (negative) slope that passes through the x-axis suggests significant and preferential damage to the hubs when compared to a healthy structural connectome.

Figure *2* provides a short explanation of basic components of graphs and prominently used metrics in studies. In short, all graphs are composed of nodes and edges; in neuroimaging studies, each node refers to a specific region of the brain and can be either structurally or functionally defined. Edges refer to the existence or strength of the connections between each node to every other node in that graph. For example, edges may be defined as the existence of white matter tracts between nodes or the degree of functional connectivity (i.e., the level to which the signal in one region is correlated to the signal in another region) between each pair of brain regions. Once nodes are defined and edges are calculated for all node pairs, these values are represented in the form of a matrix, and graph analysis metrics are calculated from the matrix to describe the properties of the network.

Although a variety of graph analysis metrics can be used to describe network properties, they can be divided into the following categories: measures of segregation (i.e., the extent to which information is processed locally within a small region), measures of integration (i.e., the extent to which information is processed across spatially distributed regions), and measures of centrality (i.e., properties of nodes that describes its importance within the network).

1.5   Graph Theory Studies in Healthy Brains

Research studies examining brain networks have demonstrated the existence of two properties in healthy human brains: small-world topology (Figure 3) and the existence of hubs. Small-worldness is a network structure defined by the existence of predominantly short-distance connections and a few long-distance connections. Small-world networks are considered to strike the optimal balance of segregation and integration, where transfer of information between regions can be completed efficiently with relatively low wiring costs. Wiring cost refers to the metabolic cost of maintaining connections; in the context of a human brain, the maintenance of

white matter tracts requires biological resources (e.g., energy/glucose, proteins). Long distance white matter tracts are more biologically costly to maintain than short white matter tracts; as such, there are upper limits to the number of long distance that can exist in the system. Loss of small-world network structure is commonly reported in network studies of clinical groups including AD and schizophrenia (Bullmore & Sporns, 2009).
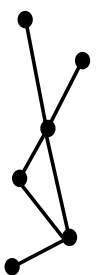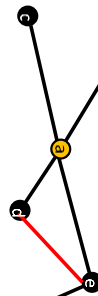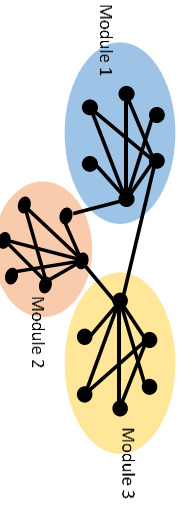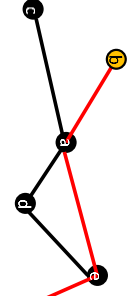
Category	Metric		Definition	Example	Interpretation Within Neuroimaging Context
Basic components	Node	Regions	Nodes are represented by black dots in the diagram to the right		Nodes are defined by the researcher.
	Edge	Relationships between nodes pairs	Edges are represented by the black lines connecting node pairs		Edges are defined by the researcher.
	Density		Proportion of existing edges in the network out of the total possible edges	There are 15 potential edges in a network made of 6 nodes. The network on the right has 6 existing edges. The density of the network is $6/15 = 0.4$	Density is a property of the network
Measures of segregation	Clustering coefficient, C		The probability that the neighbors of the node are also connected to each other in the form of a triangle	Clustering coefficient of node $a = 1/6$. Node a's neighbors are b, c, d, and e. Only 1 node pair (e-d) is connected and form a triangle with node a (marked in red). 6 total node connections are possible with node a's neighbors (b-c, c-d, e-d, b-e, c-e, b-d).		A network with a high clustering coefficient is thought to represent a network with high level of processing that is completed locally within small region.
	Modularity, Q		Existence of communities that have more connections with one another than expected in a random null model		High modularity is thought to suggest the existence of many modules (communities of nodes) with specialized functions.
Measures of integration	Path Length, L		The fewest # of edges between two nodes	Path length from node b to $f = 3$ (marked in red). Characteristic path length is equal to the average of all the distances between each node and all other nodes.	Low characteristic path length is thought to relate to high levels of global processing (i.e., information is processed through spatially distributed regions across the brain)
	Global Efficiency, E_{glob}		Inverse of path length, L	Efficiency from node b to f= Inverse of 3= 1/3	High global efficiency suggests high capacity for parallel processing, and high levels of global processing.
Measures of centrality	Betweenness Centrality, $B*$,		# of shortest paths that must pass through the node		High betweenness centrality suggests a node that is important for processing in that network, and has a large influence on the transfer of information throughout the network
	Hub disruption index		Summary measure describing the preferential impact to hubs.	If the hub disruption index is calculated from the betweenness centrality values, a plot is created where the x axis represents the average betweenness centrality for each node in the healthy control group, and the y axis represents the difference between the average betweenness centrality for each node between the patient vs. the average healthy group. The slope of the best-fit line through this data is the hub disruption index.	A high (negative) slope that passes through the x-axis suggests significant and preferential damage to the hubs when compared to a healthy structural connectome.

Figure 2. Definitions and examples of graph analysis metrics.
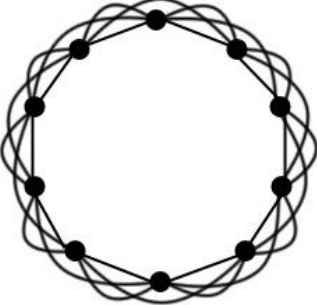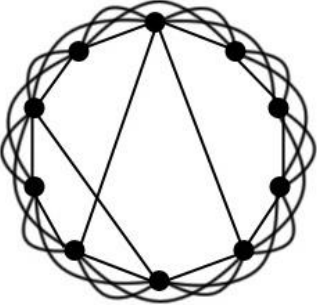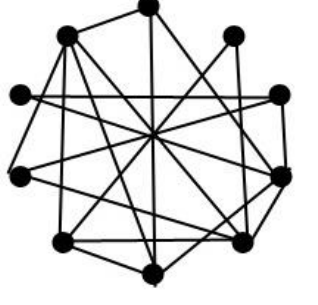
	Ordered/Regular Network	**Small World Network**	**Random Network**
Characteristics	**All connections are local**; each node is connected only to its nearest neighbors. No long distance connections.	**Most connections are local, with a few long distance connections**. Strikes the optimal balance of segregation and integration, with high global information processing efficiency despite low wiring costs	Connections between nodes are random with **equally probable local and long-distance connections**
Average Path Length	**High** path length. Ex: A large number of steps are required to travel to distal nodes.	**Short** path length. Ex: A short number of steps are required to travel to distal nodes. Long distance connections are used as 'shortcuts'.	**Short** path length. Ex: A short number of steps are required to travel to distal nodes.
Clustering Coefficient	**High** clustering coefficient; only local, repetitive connections exist.	**High** clustering coefficient, as the vast majority of connections are local	**Low** clustering coefficient, as nodes are connected randomly
Wiring cost	**Very low** wiring costs; the cost to maintain local connections is low.	**Low**; given that most connections are local (with only a few long distance connections) wiring cost is kept relatively low	**High** wiring costs; maintaining all of these long distance connections in the network is costly
Global efficiency°	**Low**; information transfer to distant nodes is slow/inefficient	**High**; information can transfer to distant nodes with ease due to given the existence of several long-distance 'shortcuts'	**Very high**; information can transfer to distant nodes with ease

Figure 3. Descriptions of three different types of networks.
Nodes are represented with black circles and edges are represented with black lines. °High characteristic path length is inversely proportional to global efficiency. High path length suggests low global efficiency, while low path length suggests high global efficiency.

Research has also demonstrated the existence of hubs (van den Heuvel & Sporns, 2011; van Straaten & Stam, 2013). Human brains exhibit a power law distribution of nodes; the vast majority of nodes in a network have a low number of connections to other nodes, but several nodes have an exceptionally high number of connections to other nodes and are integral for integrative processing. These highly connected nodes are defined as hubs. A network that follows a power law distribution of nodes ensures resilience to "random attacks", as random

attacks to the network will most likely affect nodes with low degree that are less important for network functioning. Studies using computational models of networks show that deleting a node with low degree results in networks that can continue to function and maintain its global processing efficiency. However, when hubs are targeted deliberately and deleted from the network, the network exhibits drastic decreases in levels of global efficiency.

Although there is some variability across the literature regarding regions that are hubs in the human brain due to methodological variation across studies, cortical regions such as the bilateral precuneus, superior frontal gyrus, insular cortex, superior frontal gyrus, superior parietal cortex, medial parietal cortex, and isthmus of the cingulate cortex are commonly implicated as regions of strong importance to the network. Subcortical structures such as the hippocampus, putamen, and thalamus are also suggested to be hubs (Hagmann et al., 2008; Li et al., 2013; van den Heuvel & Sporns, 2011). Overactivity and underactivity of these hubs have been demonstrated in network studies of clinical populations (Crossley et al., 2014a) and may represent a final common pathway in the disease process of *all* neurological disorders (van den Heuvel & Sporns, 2013).

Studies of graph theory in healthy individuals in relation to neuropsychological testing has shown that more efficient large-scale networks are correlated with higher IQ scores (van den Heuvel, Stam, Kahn, & Hulshoff Pol, 2009) even after controlling for age and gender (Li et al., 2009).

1.6   Graph Theory in Clinical Populations

Research studies of other clinical populations have demonstrated the utility of graph theory when evaluating brain networks. Studies of patients with stroke, schizophrenia, Alzheimer's Disease, traumatic brain injury (TBI), epilepsy, and multiple sclerosis have shown

disruptions in measures of segregation, integration, centrality, and small-world properties of networks when compared to healthy adults (Aerts, Fias, Caeyenberghs, & Marinazzo, 2016; Bullmore & Sporns, 2009).

Neurological insults, both focal and diffuse, are associated with significant changes to the topological structure of the network. A study of patients with stroke found reduced levels of communicability structural networks indicated decreased communicability in regions around the lesioned area, as well as regions in the healthy contralesional hemisphere, suggesting more difficulties in information transfer through the network (Crofts et al., 2011). Lower measures of integration were found in two separate studies that evaluated structural networks of patients with cerebral amyloid angiopathy and patients with silent lacunar infarcts in the basal ganglia territory (Reijmer et al., 2015; Tang et al., 2015). Multiple studies examining structural networks of patients with chronic TBI (which is associated with both focal and diffuse damage to the brain) consistently have shown decreases in measures of integration, decreases in measures of segregation, and decreases in measures of centrality compared to healthy structural networks (Aerts et al., 2016).

Studies have also shown that topological properties of the structural network are related to the degree of impairment. For instance, studies of patients with TBI have shown that lower global efficiency is related to lower executive functioning (Caeyenberghs et al., 2014; Yuan, Wade, & Babcock, 2015). Another study of adolescents with congenital heart disease showed that global network properties mediated the neurocognitive differences between the patient and control groups and measures of IQ, academic achievement, memory, executive functioning and visual-spatial functioning (Panigrahy et al., 2015). These studies suggest that graph theory

metrics are sensitive to brain network differences in several clinical populations, and, furthermore, are significantly correlated with behavioral measures.

Hubs also appear to be a very important feature of many clinical diseases and may represent a common pathway for all diseases. Hubs are disproportionately and consistently affected across different clinical populations due to their purported importance in the overall network; in chronic stages of the injury, these regions often show significant decreases in measures of centrality (Crossley et al., 2014b). A meta-analysis of graph theory studies across 26 different brain disorders found that abnormalities were most likely to be located in the hubs of the human connectome. Although the identity and location of the specific hubs themselves varied across different disorders (e.g., hubs affected in schizophrenia were located in the frontal and parietal lobes, while hubs affected in Alzheimer's were located in the temporal lobe), studies overwhelmingly found that hubs were implicated in these disorders. Studies of patients with TBI also have demonstrated that properties of these hub regions, particularly the superior frontal gyri and superior parietal gyri, are related to behavioral outcomes (Caeyenberghs et al., 2012; Fagerholm, Hellyer, Scott, Leech, & Sharp, 2015; Kim et al., 2014; Yuan et al., 2015). As such, it appears that hub disruption is common in many clinical disorders regardless of pathogenesis, and that the level of disruption in hub regions relate to behavioral outcomes.

Overall, studies investigating structural network properties of clinical groups who have experienced a neurological insult (e.g., TBI, stroke) suggests that there are topological disruptions to the structural network in the shape of suboptimal integration and decreased segregation in clinical groups when compared to healthy controls. Further, clinical studies consistently identify hub regions of the structural connectome to be affected regardless of the disorder, with decreases in the measures of centrality in hub regions. Finally, metrics that

describe the integrity of the network correlate significantly with behavioral measures. Taken together, these results suggest that graph theory metrics are sensitive to structural changes that occur as a result of neurological insult, and that they demonstrate concurrent validity with behavioral measures of functioning.

Graph theory methods, however, have yet to be used to examine brain network properties of survivors of childhood brain tumors. Given that there are a multitude of factors that result in white matter disruption (i.e., the tumor itself, surgical resection, hydrocephalus, radiation and chemotherapy), and that these white matter disruptions are hypothesized to underpin cognitive and functional impairments, a network analysis framework is particularly apt when studying this clinical group, as the effects of the tumor resection and the degree of white matter disruption can be modeled as changes in edge values.

1.7   Specific Aims and Hypotheses

Accordingly, the aims of this study were to provide a complementary approach to previous neuroimaging studies on the nature of brain-behavior relationships in adult survivors of childhood brain tumors. This was achieved by employing diffusion-weighted imaging and deterministic tractography methods to model white matter tracts in the brain in adult survivors of pediatric tumors at least 4.5 years past their diagnosis. Graph theory approaches were used to determine the topological properties of the network.

To establish that this method had clinical utility in this sample, it was important to demonstrate that metrics derived from the structural network relate to behavior. For the purposes of this study, measures of executive functioning were used as the outcome variable for several reasons. First, survivors of pediatric brain tumors experience significant late effects to executive functioning skills. Survivors report more problems with task efficiency, emotional regulation and

organization when compared to sibling controls and survivors of non-central nervous system malignancies (Ellenberg et al., 2009). Deficits on performance measures of executive functioning (i.e., cognitive flexibility, working memory) are common (Edelstein et al., 2011; Hocking, Hobbie, Deatrick, Hardie, & Barakat, 2015; McCurdy, Rane, et al., 2016; McCurdy, Turner, et al., 2016; Spiegler et al., 2004; Wolfe, Madan-Swain, & Kana, 2012). Studies have also found that deficits in working memory and visuospatial planning underlie deficits in social and adaptive functioning (King, Smith, & Ivanisevic, 2015; Wolfe et al., 2013). Further, explicit training on metacognitive strategies significantly improved performance on measures of attention and concentration in pediatric brain tumor survivors (Butler & Copeland, 2002). Clearly, executive functioning is often impacted in adult survivors of pediatric brain tumors, and underlie functioning in other domains. This vulnerability in executive functioning is likely due to the fact that myelination of frontal regions that support executive functioning continues through the second decade of life (Best & Miller, 2010). As such, neurological insults and neurotoxic treatments during childhood and adolescence could contribute to poorer executive functioning.

Second, research supports that executive functioning relies on frontal-subcortical systems, rather than any one region. Its reliance on the integrity of the system makes using graph theory approaches particularly relevant. Graph theory studies in other clinical populations such as traumatic brain injury and congenital heart disease have shown that performance measures of executive functioning are related to topological properties of the structural network, where lower levels of global efficiency correlated with poorer executive functioning performance (Caeyenberghs et al., 2014; Panigrahy et al., 2015).

It is important to note that executive functioning is not a unitary construct (Stuss & Alexander, 2000; Testa, Bennett, & Ponsford, 2012). Structural equation modeling studies

investigating the factor structure of executive functioning support that it consists of a set of skills that are used for "independent, purposive and goal-directed behavior" (Busch, McBride, Curtiss, & Vanderploeg, 2005). Survivor and graph theory studies commonly use measures of cognitive flexibility as their measure of executive functioning. To stay consistent with previous studies, this study also used measures of cognitive flexibility as the behavioral outcome measure.

It is also important to note that neuropsychological tasks designed to measure the construct of cognitive flexibility all require other more basic skills. For instance, good performance on the Letter-Number Sequencing trial of the Trail Making Test requires basic skills such as visual scanning, graphomotor speed, number sequencing and letter sequencing; difficulties in any of these basic domains can contribute to poor performance on this task that may not reflect deficits in cognitive flexibility skill (Chapman et al., 1995; Savla et al., 2012). As such, a simple correlation between performance on any task purported to measure cognitive flexibility with graph theory metrics lacks specificity; it is difficult to conclude whether cognitive flexibility skill is driving the correlation, or whether some other basic cognitive skill may be contributing. To identify whether cognitive flexibility precisely is associated with structural network integrity, principal component analyses were used on several other measures that are purported to measure cognitive flexibility to isolate the variance that is associated with this domain; these will be discussed in greater detail in the methods section. Two aims were proposed to examine structural network properties of adult survivors of pediatric brain tumors. These aims and *a priori* hypotheses are detailed below:

1.7.1 *Aim 1*

The purpose of the first aim was to establish that features of the structural network are altered in adult survivors compared to healthy controls.

Hypothesis a: Measures of integration (i.e., global efficiency) would be lower in survivors when compared to controls.

Hypothesis b: Given that survivors are in the chronic stage of injury, measures of segregation (i.e., average clustering coefficient, modularity) would be lower in survivors when compared to controls.

Hypothesis c: There would be significant disruption in hub nodes such that hubs are reduced in their measures of centrality. Furthermore, hubs would be *preferentially* impacted as compared to other nodes in the network that do not hold high importance to the network.

Hypothesis d: Known risk factors, such as younger age at diagnosis, longer time since diagnosis, and higher levels of neurological and treatment risk factors (e.g., radiation, chemotherapy) would be associated with more changes to measures of integration, segregation and hub centrality.

1.7.2   *Aim 2*

The purpose of the second aim was to establish the utility of graph metrics in predicting measures of cognitive flexibility in both groups, to determine whether characteristics of the structural network underlie differences in cognitive flexibility between the two groups, and to determine whether characteristics of the structural network underpin the relationship between cumulative neurological risk factors and behavioral measures of cognitive flexibility.

Hypothesis a: Measures of integration (i.e., global efficiency), segregation (i.e., modularity, clustering coefficient) and the level of overall hub disruption (i.e., hub disruption index) would significantly correlate with measures of cognitive flexibility such that lower levels of integration, lower levels of segregation, and higher levels of hub disruption would correlate with worse cognitive flexibility.

Hypothesis b: Brain network differences would underlie differences in cognitive flexibility between the survivor and control groups. As such, the differences in cognitive functioning between survivors and controls on measures of cognitive flexibility would be mediated by network metrics.

Hypothesis c: The relationship between cumulative neurological risk factors as measured by the Neurological Predictor Scale (Micklewright et al., 2008) and cognitive flexibility would be mediated by properties of the structural network.

2   METHODS

2.1   Parent Study and Procedures

Participants for this study were recruited and data was collected as part of a larger parent study investigating long-term outcomes in adult survivors of pediatric brain tumors. The parent study was reviewed and approved by the local institutional review board, and all participants provided informed consent. Participants were originally recruited through opt-in letters, which were mailed to survivors who had been treated for a pediatric brain tumor through the Children's Healthcare of Atlanta. Letters were also mailed to survivors who had participated in a previous longitudinal study, in which they had participated as children. In all, 676 adult survivors were sent mailings. Of these, 127 survivors responded and called to set up an appointment, while 88 letters were returned. Participants were screened over the phone to ensure they were over the age of 17 and at least 4.5 years after their initial diagnosis to assess effects of long-term survivorship in adult survivors. Participants were also screened and excluded if English was not their first language, if they met criteria for pervasive developmental disorders, if they indicated a diagnosis of neurofibromatosis, or if they had experienced any other significant neurological insult (e.g.,

traumatic brain injury). Out of the 127 survivors who expressed interest, 88 total survivors met initial criteria for the study and were invited to take part in the study.

On the first day, participants arrived on site with a family member and they were interviewed to obtain medical history information. Written and signed permission was also obtained from every participant to access their medical records from Children's Healthcare of Atlanta to corroborate their diagnosis and course of treatment. Participants then underwent a comprehensive neuropsychological evaluation, a structured interview for psychological disorders (SCID-II; First, Spitzer, Gibbon, & Williams, 1997), and filled out several self-informant questionnaires. Family members filled out informant measures in a separate room. Participants were provided periodic breaks throughout the day to minimize fatigue. Finally, survivors were screened for safety to enter the MRI to determine whether they could safely participate in the imaging part of the study on a different day. Of the 88 survivors who participated in the neuropsychological portion of the study, 51 individuals participated in the imaging portion. The other 37 survivors either could not participate due to MRI safety exclusions, indicated that they were not interested in the imaging part of the study, or were lost to follow-up.

The participants arrived at the imaging center on a different day for an approximately one-hour long scan. Of the 51 survivors who were included in the imaging part of the study, qualitative and quantitative assessment revealed that 38 people had good quality imaging data for the entire diffusion scan. These 38 survivors made up the sample for this dissertation project.

Healthy adults were also recruited to serve as the comparison group for analyses. The control sample was recruited through Georgia State University's psychology department research pool, as well as fliers and advertisements in the Atlanta, GA community. All control participants completed an extensive screening for MRI safety over the phone. The control sample was

matched for age, gender and handedness with the survivor sample, and were administered the

SCID-II (First et al., 1997) to ensure that they did not currently meet criteria for current

psychological or substance abuse disorders. Additionally, all controls had no history of a

neurological illness. These steps were to ensure that the control sample truly was representative

of a healthy control sample, and that the imaging results would not be unduly influenced by

neurological or psychological disorders. Control participants followed the same procedure as

survivors; they were administered the same comprehensive neuropsychological battery and the

SCID-II on the first visit, and completed the one-hour long imaging portion of the study on a

different day. Participants were asked to provide the phone number of an informant that knew

them well (if participants selected their roommate as an informant, they were required to have

lived together for at least six months). These informants were called by the research team and

administered the informant measures over the phone after obtaining oral consent.

Survivors were paid $100 for the time and travel associated with partaking in the

neuropsychological and imaging part of the study. Community participants were also paid the

same amount, while participants recruited from the psychology department pool received class

credit for their participation on the neuropsychological testing part of the study and $50 for the

imaging part of the study.

2.2   Participants

Characteristics of the survivor sample (including brain tumor type, location, and

treatment regimen) and control sample are described below in Table 1.

Independent 2-sample t-tests were conducted on continuous demographic variables, while

Chi-square analyses were conducted on discrete demographic variables to test whether the

survivor and control groups differed significantly on these demographic factors. Mean age,

gender, and socioeconomic status were not significantly different between the two groups ($p >$ 0.05). However, the control group had a higher level of education $t(72) = 2.03$, $p = 0.046$, $d = 0.48$ and higher IQs $t(72) = 3.79$, $p < 0.01$, $d = 0.89$ when compared to the survivor group. In addition, the control group was more ethnically diverse than the survivor sample χ^2 (2, N = 74) = 10.18, $p < 0.01$.

Table 1 Demographic, diagnostic and treatment characteristics

Characteristics of control and survivor samples in imaging analyses

	Sample for Imaging Analysis	
	Controls n=38	Survivors n=38
Demographic Information		
Number of Females (%)	21 (55%)	21 (55%)
Ethnicity	34% Caucasian, 37% African-American, 11% Latino/a, 13% Asian, 5% Mixed	76% Caucasian, 11% African-American, 5% Latino/a, 3% Asian, 5% Mixed
Socioeconomic Status^		
High	21 (55%)	28 (74%)
Middle/Low	17 (45%)	9 (24%)
Mean age at examination (SD)	22.5 (4.8)	23.1 (5.0)
Mean years of education (SD)	14.5 (2.0)	13.4 (2.4)
IQ Scaled Score (SD)	111 (9)	98 (18)
Vocabulary Z-score (SD)	.63 (.74)	-.27 (1.2)
Diagnostic Information		
Mean Age at Diagnosis (SD)		9.2 (5.0)
Mean Years Since Diagnosis (SD)		14.1 (6.2)
Range (years)		4.5-30
Tumor Type (*n*, %)		
Medulloblastoma		12 (32%)
Low-grade Astrocytoma		13 (34%)
High-grade Astrocytoma		1 (3%)
Craniopharyngioma		2 (5%)
Ganglioglioma		3 (8%)
Ependymoma		2 (5%)
Other		5 (13%)°
Tumor Location (*n*, %)		
Posterior Fossa		26 (68%)
Temporal Lobe		4 (11%)

Occipital Lobe	1 (3%)
Fronto-Parietal Lobe	2 (5%)
Temporal-Parietal Lobe	1 (3%)
Hypothalamus	1 (3%)
Medulla	1 (3%)
Third ventricle/sellar/suprasellar	2 (5%)
Treatment Information	
Hydrocephalus (*n*, %)	25 (66%)
Radiation Treatment (*n*, %)	20 (53%)
Chemotherapy (*n*, %)	15 (40%)
Endocrine Disorder (*n*, %)	20 (53%)
Neurosurgery (*n*, %)	37 (97%)
Total Resection	26 (68%)
Subtotal Resection	11 (29%)
Seizure medications	3 (8%)

Note. Intelligence was measured by the Wechsler Abbreviated Scale of Intelligence (Wechsler, 1999). Seizure medications refers to individuals who were still currently on medications at the type of testing. ^SES = Current socioeconomic status was calculated using the Hollingshead Four factor Index of Social Status (Hollingshead, 1975). Family SES was used in instances where the individual reported being financially dependent on their family. High SES consisted of scores 1 and 2 on the scale, while Middle/Low SES consisted of scores 3, 4, and 5 on the scale. °1 Oligodendroglioma, 1 choroid plexus papilloma, 2 PNET Not Otherwise Specified, 1 Mixed astrocytoma/ganglioglioma

2.3   Cognitive Measures

Participants underwent a comprehensive neuropsychological battery during their first study visit. The measures that are relevant for this study are detailed below.

Measures of Cognitive Flexibility:

DKEFS Color Word Interference Test: The Color Word Interference Test consists of four different trials that differentiates between word reading, color naming, inhibitory control and cognitive flexibility (Delis, Kaplan, & Kramer, 2001). The participants were asked to name the colors of square blocks on a page (Trial 1, Color Naming), read words that are printed in black (Trial 2, Word Reading), name the color of the ink that the word is printed in while ignoring the word itself (Trial 3, Inhibition), and to switch between naming the color of the ink that the word is printed in and read the actual word based on a rule (Trial 4,

Inhibition/Switching). Each trial was preceded by a sample to ensure that the examinee understood the instructions. Trial 4 is considered a measure of cognitive flexibility, as the examinee is required to switch between inhibitory and non-inhibitory responses. The amount of time that it took to complete the task was age-normed and transformed into z-scores based on normative data. Internal consistency is moderate to high across age groups, and test-retest correlations are in the moderate to high range for most subtests *(r*=0.65 for the inhibition/switching condition).

Delis-Kaplan Executive Function System (DKEFS) Trail Making Test: The Trail Making Test consists of five different trials that differentiates between deficits in visual scanning, psychomotor speed, number sequencing, letter sequencing and cognitive flexibility (Delis et al., 2001). In each trial, examinees were presented with a large piece of paper with individual numbers and letters each encased in a circle. The participants were asked to find and cross out all threes on the page (Trial 1, visual scanning), draw a line from number to number in sequential order (Trial 2, number sequencing), draw a line from letter to letter in alphabetical order (Trial 3, letter sequencing), draw a line while switching between sequencing numbers and letters (Trial 4, number letter sequencing), and draw over a dotted line (Trial 5, motor speed) as quickly as they could. Mistakes were immediately pointed out by the examiner and the participant returned to their last correct item and continued with the measure. Each trial was preceded by a sample trial to ensure that the examinee understood the directions of the trial. Trial 4 of the Trail Making Test is considered a measure of cognitive flexibility. The amount of time that it took to complete this trial was age-normed and transformed into z-scores based on normative data. Internal consistency of this measure ranges from moderate to high across age

groups, with good total score reliability. Test-retest reliability of this measure is moderate overall but lowest for the switching condition (r=0.38).

DKEFS Verbal Fluency Test: The Verbal Fluency Test consists of three different trials and measures generative fluencies in response to phonemic (Trial 1) and semantic cues (Trial 2) (Delis et al., 2001). The third trial of this test required the participant to switch between two semantic categories. The third trial is considered a measure of flexibility as the examinee is required to switch between generating items in two semantic categories. The total number of accurate switches between semantic categories in the span of 60 seconds was measured, age-normed and transformed into z-scores based on normative data. Internal consistency is in the moderate to high range across age groups. Test-retest correlations are highest for the letter and category fluency conditions and lower for the category switching condition (r=0.36).

Measure of Psychomotor speed: Condition 5 from the DKEFS Trail Making Test (described above) was used as a measure of psychomotor speed.

Measure of Cumulative Treatment and Neurological Risk Factors: The Neurological Predictor Scale (NPS) is a measure that incorporates tumor treatment (i.e., radiotherapy, chemotherapy, neurosurgery) and other related neurological risk factors (i.e., endocrine dysfunction, hydrocephalus, seizure medications) into one cumulative score that ranges from 0 (no neurological/treatment risk factors) to 11 (highest level of risk) (Micklewright et al., 2008). Studies have documented the reliability and concurrent validity in childhood survivors (Micklewright et al., 2008; Papazoglou et al., 2008). Further, this measure is significantly associated with intelligence, adaptive functioning, processing speed, working memory and attention outcomes over and above each individual risk factor (King & Na, 2016; Taiwo et al., 2017).

2.4   Neuroimaging Parameters

Imaging data was acquired using a 3T Siemens trio MRI scanner. Participants' head movements were restricted using cushioning around the head, as well as a forehead strap. Participants were outfitted with protective earplugs to reduce scanner noise. Diffusion weighted data was acquired during a 30 gradient direction single-shot spin echo planar imaging (EPI) sequence with 60 contiguous axial slices with the following specifications: repetition time (TR) = 7700 ms; echo time (TE) = 90 ms; b = 1000 s/mm^2; voxel size = 2.0 x 2.0 x 2.0 mm; acquisition matrix = 204 x 204; sequence time = 8 min 22 secs. The diffusion encoding directions were sampled on the whole sphere. We also acquired high-resolution T1-weighted structural images for anatomical registration by collecting 176 contiguous (i.e., no gap and sharing a common border) sagittal slices. A three-dimensional magnetization prepared rapid gradient echo imaging (3D MPRAGE) sequence was used with the following parameters: acquisition matrix = 256 x 256; repetition time (TR) = 2250 ms; echo time (TE) = 3.98 ms; voxel size = 1.0 x 1.0 x 1.0 mm; field of view (FOV) = 256 mm; slice thickness = 1.0mm; flip angle = 9 degrees. We also acquired a field map with a Gradient Echo sequence to measure field inhomogeneities and compensate for geometrical distortions that result from standard EPI sequences: repetition time (TR) = 488 ms; echo time 1 (TE 1) = 4.92 ms; echo time 2 (TE 2) = 7.38 ms; voxel size = 3.0 x 3.0 x 3.0 mm; field of view (FOV) = 204 mm; slice thickness = 3.0mm; 40 slices; flip angle = 60 degrees. This field map was acquired prior to a task-based functional neuroimaging sequence approximately 20-30 minutes before the diffusion sequence. Participants remained in the scanner between the field map and diffusion sequence.

2.5   Processing steps

The processing pipeline for modelling white matter fibers in the brain, calculating network properties, and analyzing these properties through statistical analyses is represented in Figure 4. Preprocessing and analysis of diffusion-imaging data was completed through PANDA, a toolbox that combines modules from several existing programs, automates processing of diffusion datasets, and constructs a matrix based on tractography data (Cui, Zhong, Xu, He, & Gong, 2013). For this study, whole brain white matter pathways were modelled based on the diffusion data acquired from the scanner using the FMRIB Software Library (Jenkinson, Beckmann, Behrens, Woolrich, & Smith, 2012; Smith et al., 2004; Woolrich et al., 2009) and the Diffusion Toolkit (Wang, Benner, Sorensen, & Wedeen, 2007). Edge values in the networks were the average FA values of the streamlines with two end-points located in the masks of each node pair. All edge values were organized into a weighted adjacency matrix. Network properties were calculated from this matrix using the Brain Connectivity Toolbox (Rubinov & Sporns, 2010). The values representing properties of the network were used in group statistical analyses for each aim. Details regarding the programs and specific measures used for each step are discussed in greater detail in the following sections.
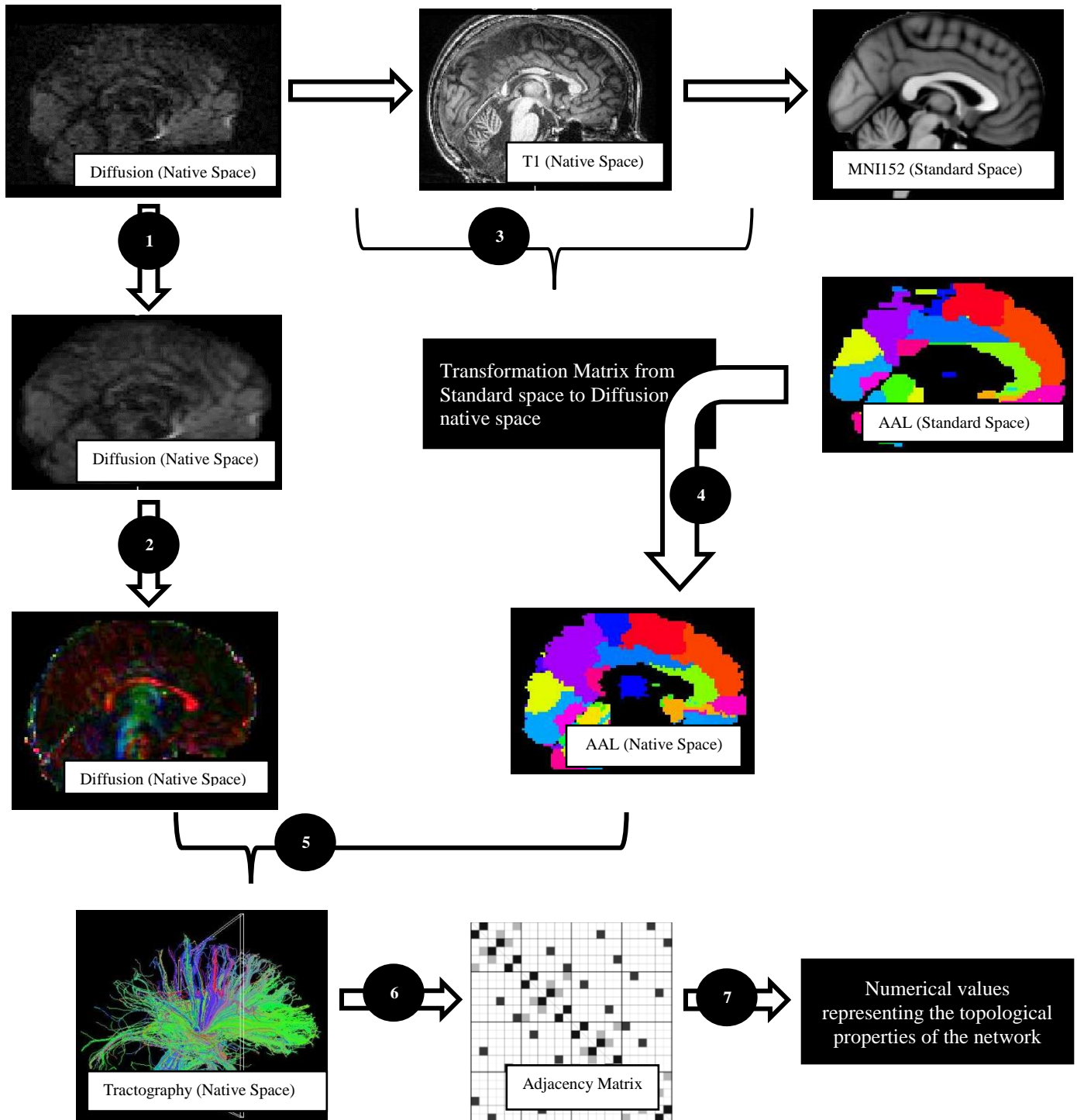
Figure 4 Processing pipeline

1. Quality assurance, preprocessing (eddy-current distortion correction), and skull-stripping of diffusion images. 2. Diffusion tensors are calculated and FA maps were generated using FSL's dtifit tool. 3. A transformation matrix was created that can be applied to go from standard space to diffusion native space by combining and inversing the matrices to transform from diffusion space to native T1 space, and from native T1 space to standard MNI space. 4. The transformation matrix from step 3 was applied to the Automated Anatomical Labeling Atlas to yield a parcellation scheme in native space. 5. Deterministic tractography was conducted using the Diffusion Toolkit software program to reconstruct white matter pathways throughout the brain. The AAL in native space was used as the nodes to construct a matrix that indicates the level of white matter connections between each node pair. 6. A weighted adjacency matrix was created for each participant which models edge values for each node pair in the network. 7. The Brain Connectivity Toolbox was used to determine the topological properties of the network; these numerical values was used in SPSS for all subsequent group-level analyses.

2.5.1   *Preprocessing*

Before imaging data was processed, each person's diffusion-weighted images underwent visual and quantitative inspection for quality assurance. First, visual inspection was conducted using the FSLview filmstrip to check for distortion, artifact, or clear movement that may render the image unusable for analysis.

The images that passed inspection underwent correction for eddy current distortion and subject movement using the "eddy" tool from FSL (Andersson & Sotiropoulos, 2016) and skull-stripped using the Brain Extraction Tool (Smith, 2002) to yield a skull-stripped diffusion weighted image. Further, the estimated translational and rotational displacement for each frame (compared to the frame that immediately preceded it) was quantified in the x, y, and z axes and summarized into one motion metric for each individual. Consistent with the approach outlined in Power, Barnes, Snyder, Schlaggar, and Petersen (2012), framewise displacement (i.e., motion) was calculated for each frame with the following empirical formula: $FD_i = |\Delta d_{ix}| + |\Delta d_{iy}| + |\Delta d_{iz}| + |\Delta \alpha_i| + |\Delta \beta_i| + |\Delta \gamma_i|$, where $\Delta d_{ix} = d_{(i-1)x} - d_{ix}$ (i.e., the level of translational displacement from one frame to the previous frame in the x-axis) and so on for each of the other parameters (translation displacement for y and z axes, as well as the rotational displacements in the x, y, and z axes). Because the output for rotational displacements were in radians, rotational displacements were converted to millimeters to be consistent with the units for translational space. This was accomplished by calculating the displacement on the surface of a sphere of radius of 50 mm, the approximate mean distance from the cerebral cortex to the center of the head.

Given that the level of motion could have a systematic impact on results, motion was compared between both groups using an independent-samples t-test, and correlations between

the level of motion and all variables were tested to determine whether motion could represent a

confound. It was determined *a priori* to use motion as a covariate for analyses that compared

between the two groups if the level of motion differed significantly between groups and

correlated significantly with an outcome measure.

The final preprocessing step involved calculating diffusion tensors and generating FA

maps using FSL's dtifit tool.

2.5.2   Tractography and Network Construction

A single file with non-overlapping nodes in native diffusion space is required to filter the

whole brain file to only include streamlines that pass through each region of interest (i.e., nodes).

For this study, the Automated Anatomical Labeling Atlas (Tzourio-Mazoyer et al., 2002) was

used as the parcellation scheme to indicate nodes of interest for this study. This atlas, which is in

standard MNI space, divides the brain into 120 distinct cortical and subcortical regions (listed in

Table 2); there are 47 anatomical cortical volumes of interest in each hemisphere and 26

subcortical volumes. Each of these regions defined a node in the network analyses, while average

fractional anisotropy between each node pair represented edges in the network analysis.

Table 2 ID #s and regions in the Automated Anatomical Labeling atlas

ID #	Brain region name	ID #	Brain region name	ID #	Brain region name
1	Left precentral gyrus	41	Left hippocampus	81	Left thalamus
2	Right precentral gyrus	42	Right hippocampus	82	Right thalamus
3	Left superior frontal gyrus, dorsolateral part	43	Left parahippocampal gyrus	83	Left transverse temporal gyri
4	Right superior frontal gyrus, dorsolateral part	44	Right parahippocampal gyrus	84	Right transverse temporal gyri
5	Left middle frontal gyrus	45	Left amygdala	85	Left superior temporal gyrus
6	Right middle frontal gyrus	46	Right amygdala	86	Right superior temporal gyrus
7	Left opercular part of inferior frontal gyrus	47	Left calcarine sulcus	87	Left superior temporal pole
8	Right opercular part of inferior frontal gyrus	48	Right calcarine sulcus	88	Right superior temporal pole
9	Left area triangularis	49	Left cuneus	89	Left middle temporal gyrus
10	Right area triangularis	50	Right cuneus	90	Right middle temporal gyrus

11	Left orbital part of inferior frontal gyrus	51	Left lingual gyrus	91	Left middle temporal pole
12	Right orbital part of inferior frontal gyrus	52	Right lingual gyrus	92	Right middle temporal pole
13	Left rolandic operculum	53	Left superior occipital	93	Left inferior temporal gyrus
14	Right rolandic operculum	54	Right superior occipital	94	Right inferior temporal gyrus
15	Left supplementary motor area	55	Left middle occipital	95	Left crus I of cerebellar hemisphere
16	Right supplementary motor area	56	Right middle occipital	96	Right crus I of cerebellar hemisphere
17	Left olfactory cortex	57	Left inferior occipital	97	Left crus II of cerebellar hemisphere
18	Right olfactory cortex	58	Right inferior occipital	98	Right crus II of cerebellar hemisphere
19	Left superior frontal gyrus, medial part	59	Left fusiform gyrus	99	Left Lobule III of cerebellar hemisphere
20	Right superior frontal gyrus, medial part	60	Right fusiform gyrus	100	Right Lobule III of cerebellar hemisphere
21	Left superior frontal gyrus, medial orbital part	61	Left postcentral gyrus	101	Left lobule IV, V of cerebellar hemisphere
22	Right superior frontal gyrus, medial orbital part	62	Right postcentral gyrus	102	Right lobule IV, V of cerebellar hemisphere
23	Left gyrus rectus	63	Left superior parietal lobule	103	Left Lobule VI of cerebellar hemisphere
24	Right gyrus rectus	64	Right superior parietal lobule	104	Right Lobule VI of cerebellar hemisphere
25	Left medial orbital gyrus	65	Left inferior parietal lobule	105	Left lobule VIIB of cerebellar hemisphere
26	Right medial orbital gyrus	66	Right inferior parietal lobule	106	Right lobule VIIB of cerebellar hemisphere
27	Left anterior orbital gyrus	67	Left supramarginal gyrus	107	Left lobule VIII of cerebellar hemisphere
28	Right anterior orbital gyrus	68	Right supramarginal gyrus	108	Right lobule VIII of cerebellar hemisphere
29	Left posterior orbital gyrus	69	Left angular gyrus	109	Left lobule IX of cerebellar hemisphere
30	Right posterior orbital gyrus	70	Right angular gyrus	110	Right lobule IX of cerebellar hemisphere
31	Left lateral orbital gyrus	71	Left precuneus	111	Left lobule X of cerebellar hemisphere (flocculus)
32	Right lateral orbital gyrus	72	Right precuneus	112	Right lobule X of cerebellar hemisphere (flocculus)
33	Left insula	73	Left paracentral lobule	113	Lobule I, II of vermis
34	Right insula	74	Right paracentral lobule	114	Lobule III of vermis
35	Left anterior cingulate gyrus	75	Left caudate nucleus	115	Lobule IV, V of vermis
36	Right anterior cingulate gyrus	76	Right caudate nucleus	116	Lobule VI of vermis
37	Left middle cingulate	77	Left putamen	117	Lobule VII of vermis
38	Right middle cingulate	78	Right putamen	118	Lobule VIII of vermis
39	Left posterior cingulate gyrus	79	Left globus pallidus	119	Lobule IX of vermis
40	Right posterior cingulate gyrus	80	Right globus pallidus	120	Lobule X of vermis (nodulus)

The AAL's parcellation scheme was chosen for several reasons. First, this atlas is commonly used in other papers utilizing graph theory to study structural network properties in other clinical populations. Using the same atlas consistently allows for more direct comparisons of results (especially related to measures of global integration) across different studies. This atlas also includes both subcortical and cortical regions as nodes. Given that subcortical structures are included as hub regions and that they have important roles in the systems required for executive functioning, inclusion of an atlas that has both subcortical and cortical regions is essential. Finally, research has shown that graph theory measures are more reliable when there is a high number of nodes; several methodological researchers have suggested that there should be at least 100 nodes to obtain reliable results (van Straaten & Stam, 2013). The AAL, with its 120 regions, fits this requirement.

To use the AAL (which is in high resolution standard space) in native diffusion space, images from native diffusion space were co-registered to each person's whole-brain T1 image using a linear transformation. The epi_reg tool was used to register diffusion images to T1-weighted images while correcting for EPI distortions using the fieldmap acquired with a gradient-echo sequence and processed using the Fsl_prepare_fieldmap tool in FSL (Jenkinson, Bannister, Brady, & Smith, 2002; Jenkinson & Smith, 2001). The epi_reg tool registered the field map to the structural image and used the registered field map image to correct for distortions while simultaneously registering the diffusion image to the structural image using linear registration methods.

This co-registered image was then registered to a high resolution standard space using a combination of linear and nonlinear transformations. These matrices were inversed and

combined to yield a matrix that could be applied to the standard space AAL image to warp all nodes into each person's native diffusion space.

Next, deterministic tractography was performed using the Diffusion Toolkit option in the PANDA program on the preprocessed data to construct all possible fibers within the brain in native diffusion space (Wang et al., 2007). This whole brain tractography file was constructed by placing a seed in all white matter voxels and linearly propagating lines from each seed based on the principal direction of the vector in that voxel. Each line was propagated by 0.25mm to the next 'point' in space, at which point the process was repeated. Each of these streamlines was terminated when certain criterion were reached (i.e., FA < 0.15 or when the angles of the paths were greater than 55 degrees). All possible streamlines were constructed from each seed region for a whole brain tractography file. The FA threshold of 0.15 was used as one of the termination criterion as prior research has shown that survivors have overall lower white matter integrity when compared to age-matched controls. The cingulum in the cingulate gyrus part was visualized for several participants using Trackvis based on ROI protocols from prior research (Wakana et al., 2007) to ensure that the whole brain tractography could follow the trajectory of a long distance white matter tract (Appendix).

The transformed AAL image was used to filter the whole brain file to only include streamlines that passed through each node pair. Specifically, streamlines with two end-points within the masks of each given node pair were considered to link the two nodes. The average FA of all the voxels along streamlines linking two nodes were considered the edge weight value for that node pair.

2.5.3   Network Properties

An adjacency matrix was constructed, where each node was represented in rows and columns and edge values were entered into cells of the intersecting row and column of the corresponding node pair. The Brain Connectivity Toolbox was then used to calculate the topological properties of each participant's matrix. Measures of properties of nodes (i.e., betweenness centrality) and properties of the overall network (i.e., density, global efficiency, average clustering coefficient, modularity) were identified for each person. A short description of

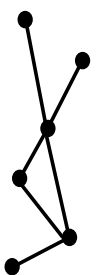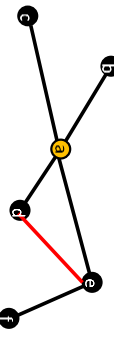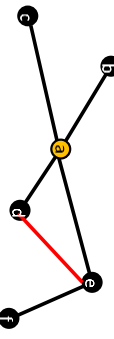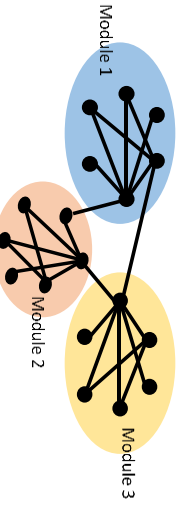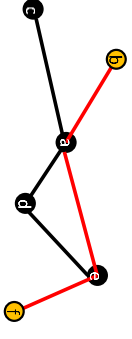the relevant metrics is provided below and in

Category	Metric	Definition	Example	Interpretation Within Neuroimaging Context
Basic components	Node	Regions	Nodes are represented by black dots in the diagram to the right	Nodes are defined by the researcher.
	Edge	Relationships between nodes	Edges are represented by the black lines connecting node pairs	Edges are defined by the researcher.
	Density	Proportion of existing edges in the network out of the total possible edges	There are 15 potential edges in a network made of 6 nodes. The network on the right has 6 existing edges. The density of the network is $6/15 = 0.4$	Density is a property of the network
Measures of segregation	Clustering coefficient, C	The probability that the neighbors of the node are also connected to each other in the form of a triangle	Clustering coefficient of node a = 1/6. Node a's neighbors are b, c, d, and e. Only 1 node pair (e-d) is connected and form a triangle with node a (marked in red). 6 total node connections are possible with node a's neighbors (b-c, c-d, e-d, b-e, c-e, b-d).	A network with a high clustering coefficient is thought to represent a network with high level of processing that is completed locally within small region.
	Modularity, Q	Existence of communities that have more connections with one another than expected in a random null model	Module 1 Module 2 Module 3	High modularity is thought to suggest the existence of many modules (communities of nodes) with specialized functions.
Measures of integration	Path Length, L	The fewest # of edges between two nodes	Path length from node b to f = 3 (marked in red). Characteristic path length is equal to the average of all the distances between each node and all other nodes.	Low characteristic path length is thought to relate to high levels of global processing (i.e., information is processed through spatially distributed regions across the brain)
	Global Efficiency, E_{glob}	Inverse of path length, L	Efficiency from node b to f= Inverse of 3= 1/3	High global efficiency suggests high capacity for parallel processing, and high levels of global processing.
Measures of centrality	Betweenness Centrality, $B*$,	# of shortest paths that must pass through the node	Low Medium High	High betweenness centrality suggests a node that is important for processing in that network, and has a large influence on the transfer of information throughout the network
	Hub disruption index	Summary measure describing the preferential impact to hubs.	If the hub disruption index is calculated from the betweenness centrality values, a plot is created where the x axis represents the average betweenness centrality for each node in the healthy control group, and the y axis represents the difference between the betweenness centrality for each node between the patient vs. the average healthy group. The slope of the best-fit line through this data is the hub disruption index.	A high (negative) slope that passes through the x-axis suggests significant and preferential damage to the hubs when compared to a healthy structural connectome.

Figure *2* in the introduction. More detailed information about the mathematical definitions of network measures is provided in Rubinov and Sporns (2010).

Basic Properties of the Network:

Density: Density is a basic characteristic of the network and describes how many existing edges there are in the network out of the number of total possible edges. Methodological studies have demonstrated that other network metrics change as a result of density rather than the properties of the local or global network (van Straaten & Stam, 2013). As such, density was kept equal for both groups when constructing the adjacency matrices for both survivors and controls to account for differences in network densities before further comparison analyses. The average density for the entire sample (i.e., survivors and controls) was calculated and used as the threshold for each participant's network matrices to preserve the same proportion of the strongest weights across all individuals.

Measures of Integration:

Global efficiency: Global efficiency reflects a characteristic of the overall network. It is calculated as the inverse of the path length (the average of the fewest number of edges between all node pairs in the network). A network with a high global efficiency suggests high capacity for parallel processing and thus higher levels of global processing.

Measures of Segregation:

Clustering coefficient: The clustering coefficient is a measure of segregation and represents the probability that the neighbors of a node are also connected to each other in the form of a triangle. A node with high clustering coefficient suggests high levels of local processing in that node. The clustering coefficient across all nodes are averaged for an overall measure of segregation in the structural network.

Modularity: Modularity is also a measure of segregation. It is defined as the existence of communities that have more connections with one another (i.e., high number of within-group links) than is expected in a random model. High modularity values suggest the existence of communities of nodes that have specialized functions.

Measures of Centrality:

Betweenness Centrality: Betweenness centrality is a measure of centrality and is calculated as the number of shortest paths that must pass through that node. A node with a high betweenness centrality suggests that the node is important in the overall network and has a large influence on the transfer of information throughout the overall network. Nodes with the highest betweenness centrality and node degree values are often deemed hubs.

Hub Disruption Index (HDI): The hub disruption index is calculated using other measures of centrality (see Figure 5). In this project, betweenness centrality was used to calculate the hub disruption index. A plot was created where the x axis represents the average betweenness centrality for each node in the healthy control group, and the y axis represents the difference between the betweenness centrality for each node between the survivor vs. the average healthy group. The slope of the best-fit line through this data is the hub disruption index. A high (negative) slope that passes through the x-axis suggests significant and preferential damage to the hubs when compared to a healthy structural connectome. In contrast, if there are random changes to nodes (i.e., non-preferential damage to hubs) with respect to these measures of

centrality, the slope of this line would not be significantly different from zero (Termenon,

Achard, Jaillard, & Delon-Martin, 2016).

Figure 5 Hub disruption index calculation from betweenness centrality values

2.6   Statistical Analyses

Statistical analyses are detailed in the following sections, each corresponding to the three

Betweenness Centrality (BC) of all nodes in healthy controls
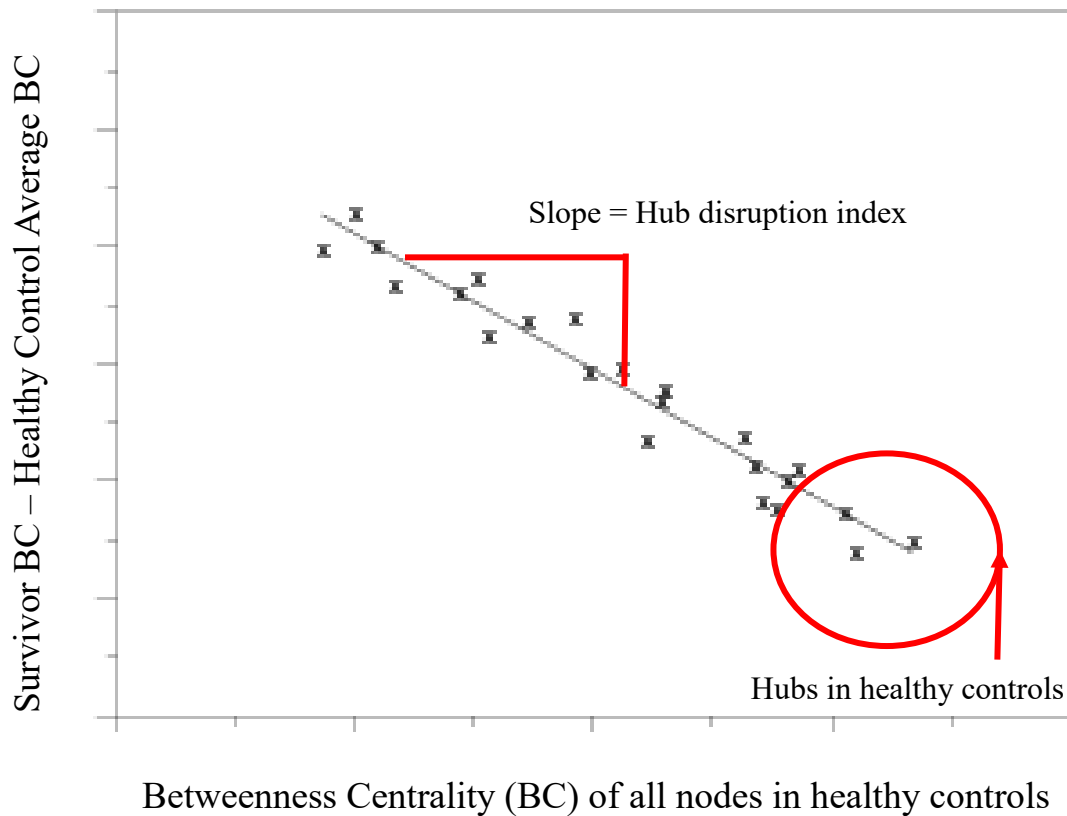
aims of the study. Given that there is a high number of statistical comparisons and tests being

conducted, adjustments were made for multiple comparisons to reduce the potential for Type I

error. Since there were four graph theory metrics that were analyzed for each hypothesis, results

were considered significant at a *p*-level equal to or below 0.0125 (i.e., $p \leq 0.05/4$).

2.6.1   Aim 1

The purpose of the first aim was to characterize structural network properties in adult survivors as compared to healthy controls.

A series of independent two-sample t-tests were conducted on the following metrics: global efficiency, average clustering coefficient, and modularity. Rather than compare measures of centrality for each individual node between groups (which increases the chance for Type I error), the hub disruption index was used as a measure of preferential damage to hub nodes. This index was calculated for each survivor based on the betweenness centrality metric for every node in the network, and a one-sample t-test was conducted on the average hub disruption values among the survivor sample to test whether this index was significantly different from zero.

Lastly, bivariate Pearson correlations were conducted to test whether risk factors identified in previous literature were associated with disruptions to the structural connectome. Specifically, younger age at diagnosis, longer time since diagnosis and higher NPS scores were expected to be significantly related to lower levels of global efficiency, lower clustering coefficient, lower modularity, and a higher hub disruption index.

2.6.2   Aim 2

The purpose of the second aim was to establish the utility of these graph metrics in predicting cognitive flexibility in both groups. To statistically test this aim, metrics from the network described in Aim 1 were correlated with age-normed z-scores from the Inhibition/Switching Trial of the Color-Word Interference Test. This task was chosen to represent the main measure of cognitive flexibility because it had the best psychometric properties out of all three cognitive flexibility measures based on the data provided in the DKEFS manual. It was hypothesized that lower levels of global efficiency, lower clustering

coefficient, lower modularity, and a higher hub disruption index would be significantly correlated with worse scores on this task. Based on previous studies that global efficiency is most robustly related to cognitive measures in structural network studies in both healthy individuals and in clinical groups it was hypothesized that global network efficiency would have the highest correlations with measures of cognitive flexibility when compared to other metrics (Caeyenberghs et al., 2012; Rubinov & Sporns, 2010; Wen, He, & Sachdev, 2011).

To determine whether cognitive flexibility truly drove the correlation between performance on the inhibition/switching trial and graph theory metrics, a principal component analysis was conducted on three different cognitive flexibility measures in the DKEFS to extract the latent cognitive flexibility construct underlying the performance on all three cognitive flexibility measures (i.e., Inhibition/Switching trial of the Color Word Interference Test, Letter Number Sequencing trial of the Trail Making Test, and the Category Switching trial of the Verbal Fluency test). Bivariate correlations were conducted on the factor score (i.e., the participant's performance on the speeded cognitive flexibility dimension) and the metrics of the network. Given that cognitive flexibility skill requires the integrity of frontal-subcortical brain systems, it was hypothesized that the factor scores would correlate significantly with properties of the structural network. However, since the inhibition/switching trial of the Color-World Interference Test requires basic functions that involve other areas of the brain as well (e.g., visual scanning, speeded reading, color naming), it was hypothesized that the correlations between performance on this measure and graph theory metrics would be higher than the correlations between the factor scores and the properties of the structural network.

Further, it is important to note that each of the three DKEFS measures were completed under a time limit. Thus, it is possible that the speeded cognitive flexibility dimension extracted

from the principal components analysis of all three measures may reflect shared method variance. To test that cognitive flexibility is associated with metrics from the structural network outside of the demands of simple speed, partial correlations were conducted between the factor scores and the properties of the structural network after removing the variance associated with simple graphomotor speed (i.e., score on Trial 5 of the Trail Making Test). A significant partial correlation would provide more support for the hypothesis that the properties of the connectome are associated specifically with cognitive flexibility.

The second hypothesis of aim 2 was that the differences in brain network properties would underlie the cognitive differences between survivor and control groups. The graph theory metric that most highly correlated with scores from the Inhibition/Switching Trial of the Color-Word Interference Test was used as the mediator between group membership (i.e., survivors vs. controls) and cognitive flexibility.

The SPSS "indirect" script was used to test the mediation model with group membership (survivors vs. controls) as the independent variable, the Inhibition/Switching Trial performance as the dependent variable, and graph theory metrics as the hypothesized mediator. Given the relatively small sample size and the concerns of the Baron and Kenny (1986) model and Sobel test for detecting effect sizes in small samples, bootstrapping was employed with 10,000 samples (Preacher & Hayes, 2004). Bootstrapping can estimate effect sizes accurately with small samples and skewed distributions by resampling with replacement. An effect is deemed significant if the resulting 95% confidence interval of the indirect effect of the independent variable on the dependent variable does not include zero. Given that this approach can increase the likelihood of Type I error, a Test of Joint Significance was also conducted; if the paths of the regression between the independent variable and the hypothesized mediator (path 'a'), as well as the

regression between the hypothesized mediator and the dependent variable (path 'b') were

significant, then the indirect effect was also considered statistically significant. If the structural

network metric emerged as a significant mediator in this model, this would suggest that

structural network properties underlie cognitive flexibility differences between groups.

The third hypothesis was that the relationships between treatment severity and cognitive

outcomes would be mediated by properties of the structural network. The same bootstrapping

and Test of Joint Significance methods used in the prior hypothesis step was utilized to test the

mediation model for this aim. The network metric most significantly related to performance on

the Inhibition/Switching trial of the Color-Word Interference Test was used as the mediator in

the model. Scores on the NPS served as the independent variable, while performance on the

inhibition/switching trial of the Color-Word Interference Test served as the dependent variable in

this model. If the structural network metric emerged as a significant mediator in this model, this

would suggest that treatment factors are related to cognitive flexibility performance through

structural network properties.

3   RESULTS

3.1   Motion

Mean average displacement for each frame was 0.60 mm (SD = 0.16) for controls and

0.65 mm (SD = 0.16) for survivors. Average framewise displacement did not differ significantly

between the two groups, $t(74) = 1.25$, $p = 0.22$, $d = 0.29$. Motion did not correlate significantly

with any of the graph theory metrics or performance on any of the cognitive flexibility measures

($p > 0.05$). Given that motion did not vary between the two groups and did not relate to the

dependent variables in the study, motion was not considered a confound and thus was not used as a covariate for proposed analyses testing each aim.

3.2 Density

Weighted matrices were derived based on the results of the whole brain tractography and density was assessed to determine whether this characteristic differed between the two groups. Average density in the healthy controls ($M = 0.29$, $SD = 0.03$) was significantly higher than the average density in survivors ($M = 0.27$, $SD = 0.03$), $t(74) = 2.44$, $p = 0.02$, $d = 0.7$. Given that differences in density can drive differences in graph theory metrics that may not reflect real differences in structural topology, each person's adjacency matrix was thresholded using the average density across the entire sample (0.279). Graph theory metrics explored in both aims were derived from these thresholded matrices.

3.3 Aim 1 Results

The purpose of the first aim was to test whether measures of integration, segregation, and centrality of the structural network were different between adult survivors and healthy controls. These results are presented in Table 3.

Table 3 Graph Theory Metrics in Survivors and Healthy Controls

Measure	Controls (n=38)		Survivors (n=38)		df	t	p	Cohen's d
	M	*SD*	*M*	*SD*				
Global Efficiency	.31	.014	.29	.019	74	3.67	.000	1.20
Avg. Clustering Coefficient	.27	.013	.26	.015	74	2.82	.006	0.71
Modularity	.25	.04	.26	.05	74	-0.30	.762	0.22
Hub Disruption Index			-.07	.14	37	-3.18	.003	0.50

Consistent with hypotheses, global efficiency and average clustering coefficient were higher in controls compared to survivors. The hub disruption index, which was calculated from

the betweenness centrality values for every node in the network, was significantly different from zero, which was also consistent with hypotheses. However, modularity did not differ significantly between the two groups.

Bivariate Pearson correlations were conducted to test whether younger age at diagnosis, longer time since diagnosis and higher NPS scores were significantly correlated with more disruptions to the structural topology. These results are presented in Table 4; scatterplots of the significant correlations in survivors are presented in Figure 6. Higher scores on the NPS (i.e., higher levels of cumulative tumor- and treatment-related risk factors) were associated with lower global efficiency and lower average clustering coefficient. These relationships were significant after correcting for multiple comparisons.

Table 4 Correlations between risk factors and graph theory metrics (n=38)

Measure	Graph Theory Metric			
	Global Efficiency	Avg. Clustering Coefficient	Modularity	Hub Disruption Index
Age of survivor at diagnosis	-0.029	.06	.11	.12
Time between diagnosis and exam	-.22	-.27	.008	-.13
Neurological Predictor Scale Score	-.61**	-.65**	.23	-.08

Note. *$p<0.05$, **$p<0.0125$ (significant after corrections for multiple comparisons).
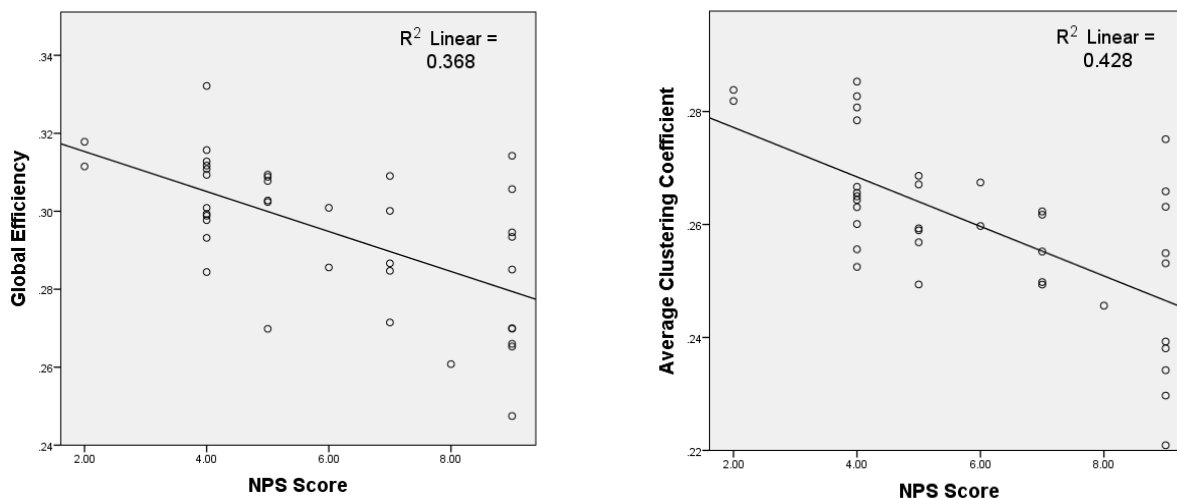
Figure 6 Scatterplots of correlations between NPS Score and graph theory metrics in survivors

3.4 Aim 2 Results

The purpose of the second aim was to establish whether graph theory metrics significantly related to performance measures of cognitive flexibility. Bivariate correlations were conducted to test whether the four graph theory metrics would be significantly correlated with age-normed z-scores from the Inhibition/Switching Trial of the Color-Word Interference Test as well as the latent "cognitive flexibility" factor derived from a principal component analysis on three different cognitive flexibility measures. Partial correlations were also conducted between the factor scores and the four graph theory metrics after removing the variance associated with simple graphomotor speed. This step was to ensure that the relationship between the cognitive flexibility dimension and properties of the structural network were not due to shared method variance in the three tasks used in the principal components analysis.

Principal components analysis was deemed appropriate for the three cognitive flexibility measures based on several checks to assumptions. First, Pearson correlation coefficients among all measures were all above 0.3, suggesting sufficient linear relationships (see Table 5). Second, the Kaiser-Meyer-Olkin Measure of Sampling Adequacy was 0.647 and over the recommended

minimum value of 0.6, indicating that the minimum cutoff was met for sample size. Last,

Bartlett's test of sphericity was significant, which suggested that the data was suitable for data

reduction, χ^2 (3) = 51.95, $p < .05$.

The first factor obtained from the principal components analysis explained 66.2% of the

variance, with an eigenvalue of 1.99; this factor was labeled "speeded cognitive flexibility".

Factor scores were computed for each subject to estimate each participant's placement on the

speeded cognitive flexibility factor. Factor loadings, which represent the relationship of each

measure to the underlying factor, are presented in Table 6.

Notably, two survivors were missing data from the Letter Number Sequencing Trial of

the Trail Making Test and the Category Switching Trial of the Verbal Fluency test of the

DKEFS. These individuals were excluded from the principal components analysis. As such, all

bivariate correlations which included the speeded cognitive flexibility factor scores were

conducted on the subsample of individuals who had data for all three cognitive flexibility

measures (i.e., all 38 controls and 36 survivors). Similarly, analyses involving the hub disruption

index and the speeded cognitive flexibility factor scores were conducted on the 36 survivors who

had complete behavioral data on all three cognitive flexibility measures.

Table 5 Correlation matrix of cognitive flexibility measures

Measure	1.	2.	3.
1. Color Word Inhibition/Switching Z-score	-	-	-
2. Trails Letter-Number Sequencing Z-score	.57	-	-
3. Verbal Fluency Category Switching Accuracy Z-score	.37	.52	-

Table 6 Factor loadings from principal components analysis

Measure	Speeded Cognitive Flexibility Loadings
Letter-Number Sequencing Z-score	.87
Color Word Inhibition/Switching Z-score	.80

Category Switching Accuracy Z-score	.77

The bivariate Pearson correlations between graph theory metrics and cognitive flexibility performance are presented in Table 7. After correcting for multiple comparisons, global efficiency was significantly correlated with performance on the Inhibition/Switching trial of the Color Word Interference Test, as well as the speeded cognitive flexibility factor derived from the principal components analysis. Global efficiency was also correlated with the speeded cognitive flexibility factor after removing the variance associated with simple motor speed. However, this relationship was not significant after correcting for multiple comparisons. Average clustering coefficient was significantly associated with performance on the inhibition/switching trial and the speeded cognitive flexibility factor. This metric was also significantly associated with the speeded cognitive flexibility factor after removing the variance associated with simple motor speed. All three of the correlations between average clustering coefficient and cognitive flexibility performance were significant after corrections for multiple comparisons.

Table 7 Correlation matrix of cognitive flexibility and graph theory metrics

Measure	Graph Theory Metrics			
	Global Efficiency	Avg. Clustering Coefficient	Modularity	Hub Disruption Index
Color-Word Inhibition/Switching Z-Score	.40**	.35**	-.12	-.15
Speeded Cognitive Flexibility Factor	.31**	.32**	-.003	-.04
Speeded Cognitive Flexibility after controlling for simple Motor Speed	.25*	.30**	-.026	.06

Note. $*p<0.05$, $**p<0.0125$ (significant after corrections for multiple comparisons).

The second hypothesis of aim 2 was that the differences in brain network properties would mediate the cognitive differences between survivor and control groups. Given that global efficiency was most highly correlated with scores on the Inhibition/Switching Trial of the Color-

Word Interference Test and had the highest effect sizes for group differences, global efficiency

was used as the mediator between group membership (i.e., survivors vs. controls) and cognitive

flexibility performance. Results of the mediation model are presented in Figure 7.

Notably, the direct effect of the independent variable group membership on cognitive

flexibility was not statistically significant. Although traditional approaches to mediation analyses

require a significant direct relationship to test for mediation, more modern statistical perspectives

posit that significant indirect effects through mediators do not depend on the presence of

statistically significant direct effects, especially within the context of a theoretically meaningful

model (Hayes, 2009).

The confidence interval for the indirect path (path c') did not include 0, and both paths a

and b in the model were significant, indicating that global efficiency mediated the differences in

cognitive flexibility performance between the two groups.
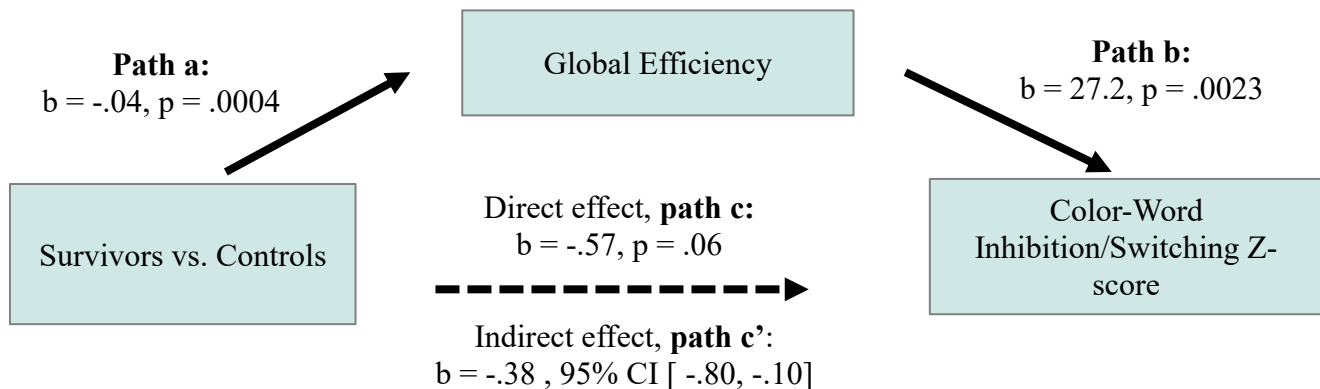
Figure 7 Global efficiency mediates cognitive flexibility differences between groups

The third hypothesis was that the relationship between treatment severity and cognitive

outcomes would be mediated by properties of the structural network. Global efficiency was also

chosen as the mediator because it was most highly correlated with scores on the

Inhibition/Switching Trial of the Color-Word Interference Test. Statistics for the mediation

model are presented in Figure 8. The confidence interval for the indirect effect of NPS score on cognitive flexibility (path c') did not include zero, and both paths and b of the model were statistically significant. These results suggest that the association between cumulative neurological risk and cognitive performance was explained by the global efficiency of the structural network.
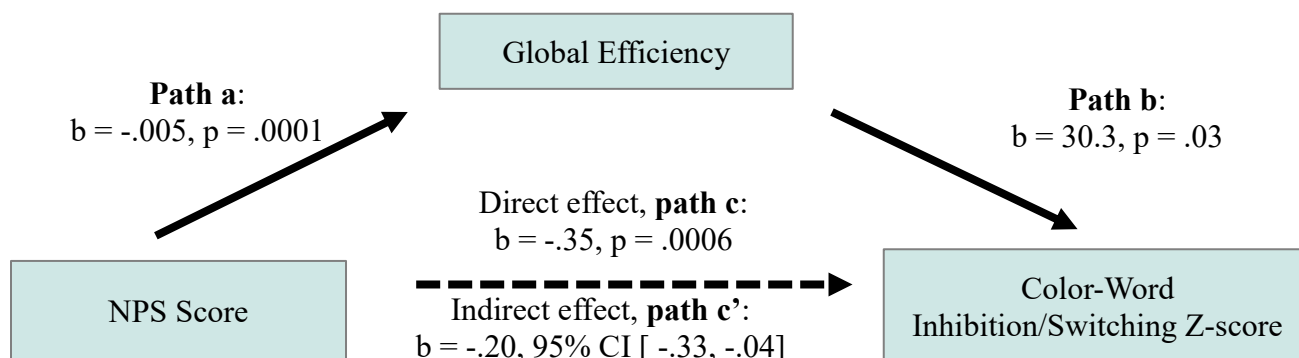
Figure 8 Global efficiency mediates the relationship between NPS and cognitive flexibility in survivors

3.5   Post-hoc Analyses

Several post-hoc analyses were conducted to test whether other variables that were potentially different between the survivor and control groups influenced the results.

3.5.1   *Mood*

One variable that may explain the differences in graph theory metrics between the two groups is the presence of depression or mood symptoms. Notably, research studies in adult survivors of pediatric brain tumors are mixed as to whether survivors experience higher levels of psychological distress compared to the general population. Some research in long-term survivors suggest minimal impact of childhood cancer on psychological well-being (Crom et al., 2014; Willard et al., 2017) while others report increased incidence of psychiatric disorders in adult survivors especially among those treated with radiation (Shah et al., 2015; Turner et al., 2009).

Independent samples t-tests were conducted on the number of current major depressive episode symptoms that were endorsed by participants on the SCID-II. Both groups endorsed very low levels of depressive symptomatology on average (Controls mean=0.06, SD = .34, Survivors mean = 0.22, SD = .72). The number of depressive symptoms endorsed did not differ significantly between the two groups, t(69)=-1.23, p = 0.22. Further, bivariate Pearson correlations revealed that the number of symptoms did not correlate with any of the graph theory metrics ($p > 0.05$). These analyses suggest that depressive mood symptoms are unlikely to explain group differences in structural network properties.

3.5.2 Education

There were significant differences between the two groups with regard to formal years of education completed. Prior research has established robust relationships between the level/quality of education and performance on neuropsychological measures in healthy individuals and clinical populations (Manly, Byrd, & Touradji, 2004; Manly, Jacobs, Touradji, Small, & Stern, 2002). Post-hoc analyses were conducted to test the potential impact of differing levels of education on the findings in this study.

Although years of education was correlated with performance on the DKEFS Color-Word Inhibition/Switching task, $r(74) = 0.23$, $p < 0.05$, formal years of education was not significantly correlated with the speeded cognitive flexibility factor score or any of the graph theory metrics. The lack of significant relationships suggests that differing levels of education between the two groups are unlikely to explain differences in structural topology.

3.5.3 IQ differences

Consistent with prior studies, estimates of IQ were correlated with features of the structural network including global efficiency, $r(74) = 0.40$, $p < 0.01$, and average clustering

coefficient, $r(74) = .39$, $p < 0.01$. Given that the control group had significantly higher IQs

compared to controls, subsamples of the two groups were created with matched IQs to determine

whether differences in graph theory metrics were still significant after accounting for these IQ

differences; these results are presented in Table 8. These subsamples consisted of 31 survivors

and 31 controls who were matched by IQ, age, gender, socioeconomic status and handedness.

Independent sample t-tests confirmed that global efficiency remained significantly different

between the two groups. A one-sample t-test also indicated that the hub disruption index was

significantly lower than 0. However, average clustering coefficient was no longer statistically

different between the two groups. The overall effect sizes from these statistical analyses were

reduced compared to the effect sizes obtained from the full sample.

Table 8 Graph theory metrics differences in subsamples with matched IQ

Measure	Controls (n=31)		Survivors (n=31)					
	M	*SD*	*M*	*SD*	df	t	p	Cohen's d
Density	.29	.03	.27	.03	60	1.65	.10	0.43
Global Efficiency	.31	.01	.30	.02	60	2.5	.01	0.65
Avg. Clustering Coefficient	.27	.01	.26	.01	60	1.74	.09	0.45
Modularity	.25	.04	.26	.05	60	-.33	.74	.09
Hub Disruption Index			-.07	.15	30	-2.8	.008	0.5

Although these analyses suggest that the topological differences between the two groups

are not fully explained by differences in IQ, it is important to note that the practice of removing

the variance associated with IQ by using subsamples or by using IQ as a covariate has been

criticized on logical, statistical, and methodological grounds. Dennis et al. (2010) presents a

series of arguments to state that using IQ as a covariate or as a variable to match groups is

"meaningless and generally unjustified." The authors argue that IQ has often used as a covariate

in studies of other neurodevelopmental conditions because it is assumed to be a meaningful static

construct that represents an innate and latent potential that *causes* individual and group

differences, but that this perspective on IQ is unfounded. For instance, research in individuals with learning disabilities do not support the notion that IQ represents a measure of potential or capacity.

In addition, the purpose of using covariates or matching procedures is to correct for selection bias. It is an established method to minimize differences that occur in two groups by chance, as even experimental conditions with random assignment procedures may result in preexisting group differences that causally affect the dependent variable. However, when studying outcomes of individuals with neurodevelopmental conditions or acquired childhood brain insults where IQ was measured after the insult, it is impossible to separate the construct of IQ from the condition meaningfully, as changes in IQ occur as a direct result of the condition. Differences in IQ that occur between the clinical sample and the healthy comparison group are not a result of a selection bias but instead represent true nonrandom preexisting population differences. Comparing outcomes in samples after matching the clinical and healthy comparison groups by IQ may result in comparing groups that are not representative of the population, as matching procedures usually remove the individuals in the clinical group who are performing more poorly. As such, matching groups by IQ removes important variance related to the very features and effects of the brain tumor and associated treatments that we are attempting to study. The finding that the effect sizes of all differences in graph theory metrics were reduced after matching the groups by IQ is unsurprising and these post-hoc analyses should be interpreted with the caveat that the subsamples may be unrepresentative samples from the populations of interest.

4   DISCUSSION

Consistent with hypotheses, the results of this study indicated that global efficiency and average clustering coefficient of structural networks were reduced in survivors compared to healthy peers matched by age, gender, handedness, and socioeconomic status. There was also evidence for preferential impact to hub regions. Further, lower global efficiency and lower average clustering coefficient were associated with higher cumulative neurological risk and poorer performance on behavioral measures of cognitive flexibility. Indeed, global efficiency mediated differences in cognitive flexibility performance between survivors and healthy peers. Global efficiency also mediated the relationship between cumulative neurological risk and cognitive flexibility performance. These results suggest that structural networks are altered in adult survivors of pediatric brain tumors and that features of these networks explain differences in cognitive flexibility performance. Post-hoc analyses suggested that these results are not due to motion artifact or to differences in education between groups. These results are highly consistent with findings from studies conducted in other clinical groups such as TBI, stroke, epilepsy, and congenital heart disease, which have shown disruptions in measures of segregation, integration, and centrality when compared to healthy adults. Prior studies also have consistently shown that metrics describing the integrity of the network significantly relate to behaviors and the degree of impairment.

Global efficiency, a measure of global integration, is thought to reflect the capacity of structural networks to allow efficient processing of information from distributed regions of the brain. The clustering coefficient is a measure of segregation that represents high levels of local processing. Brain networks of healthy individuals are associated with a balance of local and global processing in the brain so that information can be efficiently transferred across the

network while still maintaining low wiring and biological costs. Studies of healthy developing brains indicate that brain networks undergo highly dynamic changes from infanthood to late adolescence; these networks change from relatively random configurations to networks that optimize the balance between information segregation and integration. These changes support cognitive and behavioral developments (Baum et al., 2017; Cao, Huang, & He, 2017; Chen, Liu, Gross, & Beaulieu, 2013). The rapid changes occurring in structural and functional brain networks during development also render the brain more vulnerable to neurological insults. Survivors of pediatric brain tumors experience disruptions during these critical timeframes when structural and functional networks are actively being optimized for efficiency. The results of this study suggest that these network alterations persist even when survivors have grown into adulthood, as measures of both integration and segregation were reduced when compared to neurologically healthy adults of the same age. These alterations also have important consequences for behavioral outcomes, as reduced global efficiency and reduced average clustering coefficients in the network are both associated with poorer cognitive flexibility performance.

Inconsistent with hypotheses, modularity of the structural networks was not significantly different between groups, and there were no significant relationships between this metric and measures of cognitive flexibility. Lack of expected findings may be due to the parcellation scheme. The modularity metric identifies communities of nodes that are more interconnected with each other than is expected in a random model. If the nodes within a network are too large and each contain heterogeneous subregions that are highly interconnected and function as a module, then the parcellation does not have the spatial resolution to sensitively measure differences in modularity. Although the Automated Anatomical Labeling atlas has been used

frequently in other graph theory studies of clinical groups, its nodes are defined by anatomical boundaries and it is entirely possible that nodes contain subregions that are heterogeneous with regard to function and architecture.

Alternatively, it is possible that recovery prioritizes modularity of structural networks. Computational modeling studies that incorporate plasticity into their network recovery models have reported that modularity recovers over time after a lesion in the network (Stam, Hillebrand, Wang, & Van Mieghem, 2010). The cross-sectional design of this study precludes examining how modularity changes over time on an individual level. As such, longitudinal designs in future studies will be crucial to establish whether the acute and subacute stages of injury are associated with changes in modularity and whether this feature recovers as a function of time.

It is also possible that differences in modularity might exist in functional networks even during the chronic phase of injury. Other studies have identified modularity differences between patients with TBI and healthy controls when examining functional networks using resting state fMRI and EEG data (Han et al., 2014; Messe et al., 2013). Further, modularity in functional networks appear to relate meaningfully to changes in behavior. Specifically, one study showed that modularity of functional brain networks prior to a cognitive intervention program predicted the level of improvement in attention and executive functioning in patients with a brain injury (Arnemann et al., 2015). Modularity can also flexibly change in functional networks in response to a rapidly changing environment; a recent study in healthy adults demonstrated that modularity in functional networks significantly changed as individuals completed a harder working memory task when compared to a simpler vigilance task (Finc et al., 2017). The dynamic nature of functional networks may make it more suitable for understanding behavioral variation. Future studies should employ network-level analyses of functional networks such as resting state fMRI

and task-based fMRI in adult survivors of pediatric survivors to complement the findings from this study.

Further, although the present study did not find any relationships between modularity and behavioral outcomes on the group level, this does not preclude the possibility that intra-individual changes in modularity may predict outcomes. For instance, working memory capacity can be predicted by within-individual differences in functional brain network modularity in healthy adults (Stevens, Tappon, Garg, & Fair, 2012). Again, longitudinal methods could determine whether there are intra-individual changes in modularity metrics over time and whether the level of change predicts cognitive and behavioral outcomes on the individual levels.

The hub disruption index, a global measure of preferential damage to hubs based on the betweenness centrality values for each node in the network, was hypothesized to be significantly different from zero and to relate significantly to measures of cognitive flexibility. This hypothesis was partially supported. Although there was evidence that hubs were preferentially impacted compared to the other nodes in the network, the hub disruption index was unrelated to risk factor variables or any behavioral measures of cognitive flexibility. This may be due to the fact that the hub disruption index is a composite measure based on the slope of the difference scores of betweenness centrality in all of the nodes in the network and may thus be too general. Although research supports that hubs are disproportionately and consistently affected across different clinical population, the identity of these hubs does differ across different disorders. For instance, patients with schizophrenia exhibit more disruption to hubs in the frontal and parietal lobes, while patients with Alzheimer's exhibit more disruption to hubs in the temporal lobe. Although other research studies have identified significant correlations between properties of certain hubs and cognitive performance, these results rarely survive corrections for multiple

comparisons. Due to this issue, this study used one index of hub disruption to avoid running numerous statistical tests simultaneously on the betweenness centrality values for every single node in the network. However, the hub disruption index may have been too general to relate to behavior. As such, research studies which select a small number of hubs *a priori* based on theory and previous research may be better able to identify significant relationships between behavioral outcomes and local properties of these hubs. Other research studies that have used the hub disruption index have demonstrated the measure to be sensitive to differences between clinical groups and healthy peers, but did not investigate whether the hub disruption index was related to behavioral outcomes (Ridley et al., 2015; Termenon et al., 2016).

Although cumulative neurological risk was related to graph theory metrics in the survivor group, the other risk factors such as age at diagnosis and years since diagnosis did not relate significantly to any of the graph theory metrics. This does not preclude the possibility that these diagnostic variables relate to structural topology. Instead, it may be that these variables interact with other treatment variables such as presence and type of radiation. For instance, a research paper from our research lab (with an overlapping sample) indicated that age at diagnosis and radiation interacted to predict processing speed performance. Among those who had received radiation treatment, younger age at diagnosis predicted poorer processing speed. In contrast, there was no significant relationship between younger age at diagnosis and processing speed in those who had not received radiation treatment (King et al., 2017). Review of neuroimaging studies in survivors of pediatric brain tumor that have related age at diagnosis with characteristics of brain structure largely were in samples comprised solely of survivors who have experienced cranial radiation (Butler et al., 2013; Khong et al., 2003; Reddick et al., 2005; Reddick et al., 2014). Older age at diagnosis and treatment was unrelated to FA in a survivor

sample that had only experienced surgery (Law et al., 2011). As such, more complex models that incorporate interactions of age at diagnosis and time since diagnosis with treatment factors are needed to understand the nature of these risk factors on structural topology. It will also be important to incorporate variables that affect recovery, such as rehabilitation or level of family support, for a more complete model of long term survivorship (Murdaugh et al., 2017).

It is worth questioning whether graph theory metrics have specificity, as global efficiency was significantly related to multiple behavioral outcomes (e.g., IQ and cognitive flexibility). Based on the fact that many neuropsychological tasks require an integrated system to complete any given task (e.g., sensory input, process, planning and executing motor output), it is perhaps unsurprising that a measure of global integration incorporating the features of every node in the network is related to different measures of behavior. Studies of structural network properties of other clinical populations such as congenital heart disease, TBI, and stroke (among others) also have related global efficiency to a wide variety of outcomes, including postconcussive symptoms, executive functions, memory, IQ, and visual-motor integration (Caeyenberghs et al., 2014; Panigrahy et al., 2015; Reijmer et al., 2015; Yuan et al., 2015). Studies that are interested in identifying specific features of the network to dissociate between different outcomes may be more successful if they utilize metrics that describe the local properties of specific nodes/regions of interest in the network. For instance, a resting state fMRI study of 392 middle-aged and older adults found that apathy was associated with decreased measures of local properties of the anterior cingulate cortex, while depression was associated with increased measures of local properties of the anterior cingulate cortex. This study used the local network properties of one node in the network to dissociate apathy and depression in their sample (Onoda & Yamaguchi, 2015). Further, characteristics of functional networks may be better suited for understanding the

neurobiological bases of specific behaviors. Although functional networks are constrained to a certain extent by underlying structural architecture, functional networks also exhibit more flexibility and can adapt more quickly to environmental demands by reorganizing, coordinating and mobilizing different regions across the brain for various cognitive tasks (Fischer, Wolf, Scheurich, & Fellgiebel, 2014). This flexibility also raises the possibility that functional networks can attempt to compensate for some structural network deterioration. Multi-modal network approaches will be especially helpful in understanding how the brain responds and recovers over time and how these factors relate to behavioral outcomes in adult survivors of pediatric brain tumors.

The findings from this study should be considered within the context of the limitations. First, both survivor and control groups were self-selected. In the case of the survivor group, it is possible that the sample was biased towards higher functioning individuals who had the time to devote to the study and the means to transport themselves to the study site. It is also equally possible that survivors with more cognitive concerns were more likely to participate in the study. This selection process may have skewed the sample to include either higher or lower functioning survivors. Due to these factors, selection bias may limit the generalizability of the conclusions. It is also possible that survivors who were excluded from the imaging due to artifact, motion, or MRI-incompatible devices may have been lower functioning. To test this possibility, *post hoc* analyses were conducted to test whether survivors who were included in the current study had higher IQs, cognitive flexibility scores, or had experienced higher levels of cumulative neurological risks when compared to the survivors who were excluded due to various reasons (e.g., motion artifact, MRI incompatibility, disinterest). Two sample t-tests indicated that there were no differences in IQ performance, cognitive flexibility performance, or NPS scores between

the two groups ($p > 0.05$). As such, the survivors included in this neuroimaging study do not appear to be biased towards the higher functioning survivors within the larger sample of survivors who completed neuropsychological testing for the parent study.

This study was also cross sectional and thus could not provide information about causation, or about changes that occur over time; longitudinal and prospective studies will be crucial to establish time frames and causes of change. For instance, to demonstrate that structural network topology truly plays a causative role in explaining cognitive flexibility behavior, it will be important to establish that structural network changes precede behavioral changes.

Related to neuroimaging methodology, there are established limitations with the diffusion weighted imaging parameters and deterministic tractography methods used in this study. Although previous research has established some construct validity for streamline tractography methods by demonstrating that these methods agree with prominent white matter tracts found in postmortem studies, false positive and false negative streamlines can occur due to signal noise, partial volume effects and complex fiber architecture within voxels (Jbabdi, Sotiropoulos, Haber, Van Essen, & Behrens, 2015). The deterministic tractography methods used in this study assign one direction per voxel under the assumption that the direction of maximum diffusivity is an estimate of major fiber orientation. Given that there are potentially tens of thousands of axons in each voxel, assigning one direction assumes that all axons are coherently aligned in the same direction in that voxel, which is clearly inadequate especially in regions of the brain where fiber bundles cross. These approaches lead to bias in FA estimates especially in long white matter tracts (Oouchi et al., 2007). Future studies will need to employ more advanced diffusion imaging models, such as high angular resolution diffusion imaging (HARDI) or diffusion spectrum magnetic resonance imaging (DSI) to more accurately track complex fiber architecture in these

crossing fiber regions. Probabilistic tractography methods can also enhance our understanding of distributed connectivity by using algorithms to model the distribution of orientations and estimate levels of uncertainty in each voxel. It is important to note that all diffusion weighted imaging techniques are ultimately inferential methods that attempt to model white matter based on measurements of water diffusion. Even a model that perfectly measures and describes water diffusion within each voxel is unlikely to completely explain the microstructural properties of white matter tracts.

In addition, graph theory approaches to study the brain are still in development and the biological significance of these metrics is still under investigation (He & Evans, 2010). For example, research on the topological features of brains in healthy and clinical groups have largely assumed that "stronger connections are better" and have concentrated their efforts on understanding the nature of these strongest connections. Methodologically, this assumption has resulted in thresholding procedures across many different studies that preserve the strongest connections and remove the weakest connections when examining networks. However, recent research has recognized the importance of these weaker connections in explaining individual variability and symptom presentation in clinical disorders (Bassett, Nelson, Mueller, Camchong, & Lim, 2012; Santarnecchi, Galli, Polizzotto, Rossi, & Rossi, 2014). Further, there is no 'gold standard' for processing or conducting analyses in clinical populations which have potential implications for findings, as methodological choices made by the researcher on parcellation schemes, edge definitions and thresholding procedures can significantly impact the network metrics under investigation (van Wijk, Stam, & Daffertshofer, 2010). Given the lack of a gold standard, this study used similar methods and parcellation schemes as research studies

investigating structural network properties in other clinical populations. However, it is important to interpret the findings of this study within the context of the methods used.

For instance, the nodes for this study were based on the AAL parcellation which uses anatomical features to define regions of interest (Tzourio-Mazoyer et al., 2002). Although this scheme may capture important neurobiologically meaningful areas, one node may include multiple regions with heterogeneous functions. The anterior cingulate cortex, for example, exhibits a great deal of heterogeneity in both structural and functional connectivity studies but the entire region is treated as one node in the AAL (Arslan et al., 2017). Newer parcellation schemes such as the one proposed by Glasser et al. (2016) use multiple modalities to generate highly reproducible and individualized parcellations based on other features of the brain such as function, connectivity, and cortical architecture. This parcellation scheme has the added advantage of being able to automatically account for slight anatomical differences between individuals through machine-learning approaches. Although promising, this parcellation has yet to be validated or reproduced in healthy younger children or older adults, much less clinical groups whose anatomy may be altered significantly as a result of surgery and other treatments. A recent review of 10 subject level and 24 group level parcellations tested these parcellation schemes with respect to reproducibility, fidelity to underlying connectivity, agreement with task activation, myelin maps, cytoarchitectural areas, and network analysis. The review suggested that there was no clearly optimal parcellation method (Arslan et al., 2017). On a positive note, each of the tested parcellation schemes yielded graph theory metrics that performed successfully on a simple gender classification task. The authors interpreted this finding to mean that the choice of the parcellation scheme has limited impact on network analysis metrics but

acknowledged that the task was extremely simple and that future studies should examine the potential impact of different parcellation techniques on network metrics in clinical populations.

This study also used the average FA between nodes as the edge metric to extend prior research that has established that survivors of pediatric brain tumors have lower FA overall and in specific white matter tracts when compared to healthy controls. It is important to note that research studies in other clinical populations use different edge metrics such as number of streamlines and the density of streamlines as edge measures, and that differing definitions of edges can lead to variability in results. In addition, although research has shown that FA is a sensitive measure to white matter integrity, FA is a summary measure that lacks specificity to types of change. Other metrics such as mean diffusivity, radial diffusivity and axial diffusivity may be more sensitive to specific biological processes such as edema, necrosis, axonal damage, and myelin degeneration (Askins & Moore, 2008). Given that there are multiple potential mechanisms that interact to explain the late delayed effects of radiation, chemotherapy, hydrocephalus, and other brain tumor associated treatments on the brain, future studies could use metrics other than FA as edge values to explore pathology with more specificity.

Another aspect to consider is the choice to use proportional thresholding schemes to account for density differences between groups. Research has shown that graphs with different densities (i.e., the proportion of the number of existing edges out of the total possible number of edges) are difficult to compare directly because density differences in networks can result in significant differences in graph theory metrics even when networks share the same topological organization. This makes it challenging to compare networks between clinical groups and healthy same-aged peers when density may naturally change as the function of the disorder itself. There are different methods that have been proposed to deal with comparing networks of

different densities but there is no one satisfactory way to control for this issue completely, due to the fact that modeling the exact impact of density on different graph theory metrics depends on knowing the underlying topology *a priori*, which is not possible in empirical studies of clinical populations (van Wijk et al., 2010). For instance, some studies use density as a covariate to test whether graph theory metrics remain different between groups after removing the variance associated with density. This approach, however, does not fully control for the issue when density does not share linear relationships with graph theory metrics (Caeyenberghs et al., 2012). Proportional thresholding, which was the method used in this study, uses a cutoff such that the same percentage of edges are enforced for everyone's networks. This method, however, may lead to modifications of the network by ignoring significant connections in controls or by enforcing weaker connections in the clinical group (Drakesmith et al., 2015). In addition, given that controls had higher densities, using any cutoff automatically affects the control group more than the survivor group. To test whether proportional thresholding may have unduly affected the results, the same analyses were run on networks without any thresholding. The results were very similar; global efficiency and clustering coefficients remained lower in survivors compared to controls, were significantly correlated with cognitive flexibility and cumulative risk, and mediated the difference in cognitive flexibility performance between the two groups. These additional analyses suggest that the results of this study are not fully attributable to densities of networks.

Another methodological limitation in this study was the field map used to undistort the diffusion images when registering them to the T1 MPRAGE image. In the parent study, the field map was acquired before the task-based functional sequence. As the field map is based on the specific location of the head within the scanner, significant head motion between the time that

the field map is acquired and the diffusion imaging sequence can yield a field map image that does not perfectly represent the field inhomogenetities even after using linear registration techniques on the field map image to align it to the structural image. Qualitative inspections of the diffusion images after incorporating the field map did result in less distortion (see

Figure *9*). Future studies, however, should collect field maps immediately before the diffusion scan or obtain several B0 images in opposite directions to better reduce spatial distortion when acquiring imaging with Echo Planar Imaging sequences (Andersson, Skare, & Ashburner, 2003).

Figure 9 Axial and sagittal slice (a) before and (b) after field map correction
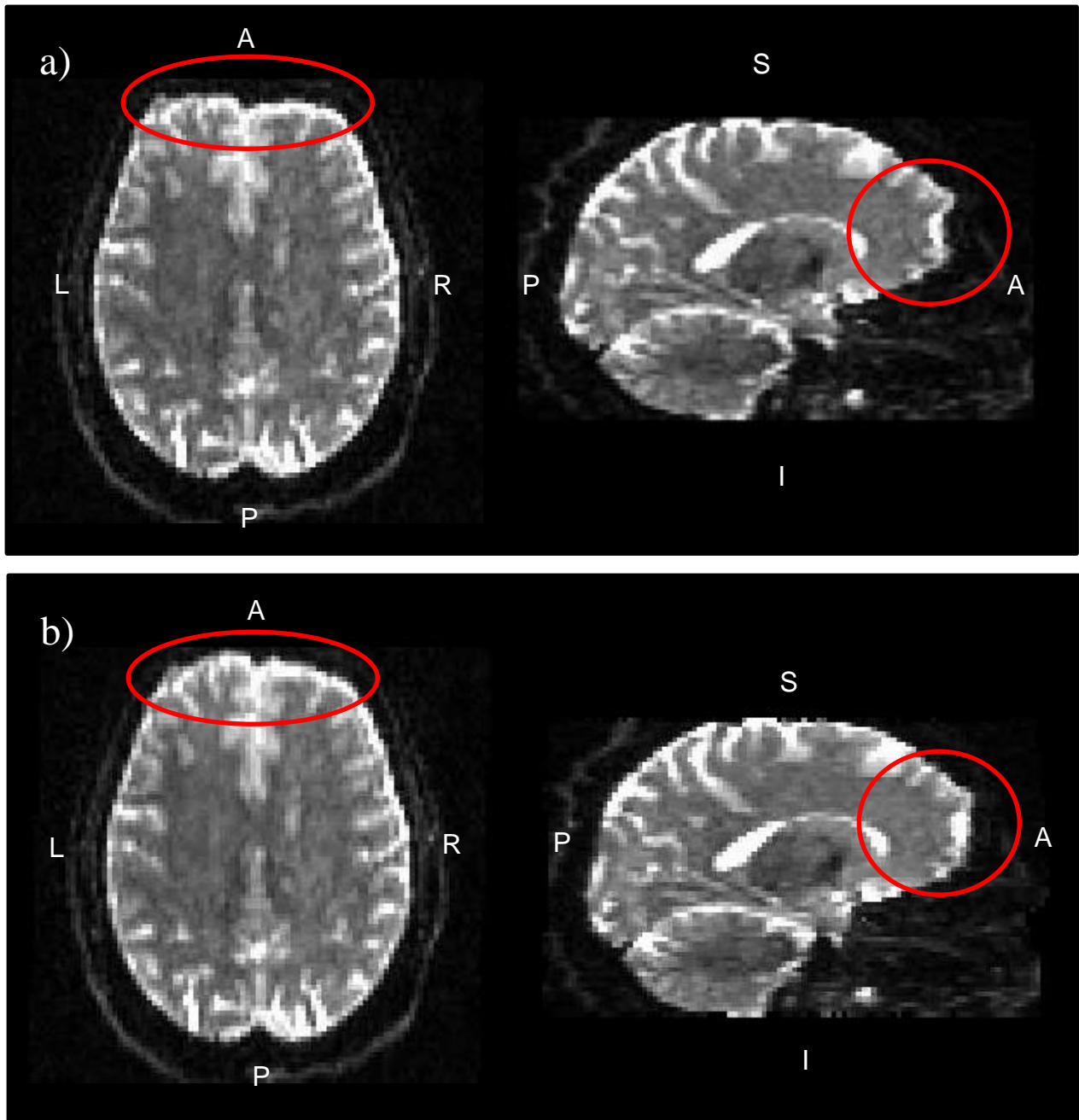
Despite these limitations, there also several strengths that are worthy of note. Like

research studies of other clinical populations, the sample studied in this group is heterogeneous

with regard to tumor type, tumor location, types of treatments and level of neurological risk. This

heterogeneity allowed for increased variance to explore the relationship between important

variables of interest and functional outcomes. There is also a respectable sample size of an

understudied population. The use of an age- and gender-matched control group allowed for comparisons between the clinical group and healthy same aged peers and to determine whether structural topology was altered in the survivor group and underpinned differences in cognitive performance between groups.

This study also explicitly considered the impact of motion on the findings. Research has suggested that differences in head motion between two groups lead to spurious but systematic differences in structural and functional neuroimaging results even when utilizing methods that attempt to compensate for motion during preprocessing steps such as spatial registration or regression of motion estimates from data (Power et al., 2012; Yendiki, Koldewyn, Kakunoori, Kanwisher, & Fischl, 2014). Using a quantitative metric of translational and rotational motion, comparing the metric between groups, and identifying whether motion related to any of the findings provides more confidence that results from this study reflect true differences between groups rather than differences in subject head motion.

Further, this is the first study to use graph theory to explore the topological properties of the structural network in survivors of brain tumors. Understanding structural topology lays the groundwork for exploring functional network organization, as functional networks are shaped and constrained to a certain extent by the underlying structure (Cao et al., 2017). Understanding the flexibility and diversity of functional network organizations within the constraints of anatomical connectivity can provide important insights into the nature of brain repair, recovery, and function following a neurological insult. Graph theory has the added benefit of being able to use dynamic modeling in a cohesive framework to understand how the features of structural and functional brain networks change over time (Hart, Ypma, Romero-Garcia, Price, & Suckling, 2016; Meyer-Base et al., 2017). Metrics derived from structural and functional brain networks

have been used as a biomarker in clinical groups such as patients with temporal lobe epilepsy to predict patients who will have better outcomes after surgery (Bonilha et al., 2015; Ji et al., 2015). Studies of this kind suggest that graph theory may even have some utility in clinical settings to guide neurosurgical planning to avoid neurological deficit, predict the efficacy of treatments, and identify patients who are at risk for poor outcomes (Castellanos, Di Martino, Craddock, Mehta, & Milham, 2013; Petrella, 2011). Although more longitudinal work is necessary in larger samples to establish that graph theory metrics have clinical value in survivors, the findings from this study suggest the potential clinical relevance of understanding structural network level properties of the brain.

5   SUMMARY

Neuroimaging techniques have been used to investigate the neurobiological underpinnings of cognitive deficits in adult survivors of childhood brain tumors. Graph theory is a quantitative method that characterizes brains as a complex system. By modeling cortical and subcortical brain regions as nodes and white matter connections between each brain region pair as edges, graph theory provides metrics that quantify the topological properties of brain networks. Given that brain tumors and medical treatments for brain tumors are known to result in disruptions to both brain regions and white matter connections and that these disruptions are hypothesized to underlie impairments in cognitive and functional outcomes, a network analysis approach was used to explore the network properties of the structural brain network. This study used diffusion-weighted imaging and deterministic tractography techniques to model structural brain networks in 38 adult survivors of pediatric brain tumors at least 4.5 years past their diagnosis (mean age=22.5 years, 54% female, mean 14.1 years post diagnosis). Nodes were

defined using the Automated Labeling Atlas parcellation scheme, and edges were defined as the mean FA of streamlines that connected each node pair. Results indicated that global efficiency and average clustering coefficient was reduced in survivors compared to healthy peers matched by age, gender, handedness, and socioeconomic status. There was also evidence for preferential impact to hub regions. Global efficiency and average clustering coefficient was significantly correlated with measures of cognitive flexibility and cumulative neurological risk. Further, global efficiency mediated differences in cognitive flexibility performance between survivors and healthy peers, as well as the relationship between cumulative neurological risk and cognitive flexibility performance. These results suggest that graph analytical metrics are sensitive in this clinical group and that differences in cognitive flexibility performance can be directly explained by properties of the structural network. Future directions include using graph theory metrics in longitudinal studies to investigate how properties of structural networks change in the acute and chronic stages of injury, exploring how structural networks repair and recover with time or as a function of pharmacological or cognitive interventions, and using graph analysis methods on the functional connectome to complement our understanding of brain-behavior relationships in adult survivors of pediatric brain tumor.

REFERENCES

Aerts, H., Fias, W., Caeyenberghs, K., & Marinazzo, D. (2016). Brain networks under attack: robustness properties and the impact of lesions. *Brain, 139*(Pt 12), 3063-3083. doi:10.1093/brain/aww194

Ahles, T. A., & Saykin, A. J. (2007). Candidate mechanisms for chemotherapy-induced cognitive changes. *Nat Rev Cancer, 7*(3), 192-201. doi:10.1038/nrc2073

Anderson, F. S., & Kunin-Batson, A. S. (2009). Neurocognitive late effects of chemotherapy in children: the past 10 years of research on brain structure and function. *Pediatr Blood Cancer, 52*(2), 159-164. doi:10.1002/pbc.21700

Andersson, J., Skare, S., & Ashburner, J. (2003). How to correct susceptibility distortions in spin-echo echo-planar images: application to diffusion tensor imaging. *Neuroimage Clin, 20*(2), 870-888.

Andersson, J. L., & Sotiropoulos, S. N. (2016). An integrated approach to correction for off-resonance effects and subject movement in diffusion MR imaging. *NeuroImage, 125*, 1063-1078.

Arnemann, K. L., Chen, A. J., Novakovic-Agopian, T., Gratton, C., Nomura, E. M., & D'Esposito, M. (2015). Functional brain network modularity predicts response to cognitive training after brain injury. *Neurology, 84*(15), 1568-1574. doi:10.1212/WNL.0000000000001476

Arslan, S., Ktena, S. I., Makropoulos, A., Robinson, E. C., Rueckert, D., & Parisot, S. (2017). Human brain mapping: A systematic comparison of parcellation methods for the human cerebral cortex. *Neuroimage*. doi:10.1016/j.neuroimage.2017.04.014

Askins, M. A., & Moore, B. D., 3rd. (2008). Preventing neurocognitive late effects in childhood cancer survivors. *J Child Neurol, 23*(10), 1160-1171. doi:10.1177/0883073808321065

Aukema, E. J., Caan, M. W., Oudhuis, N., Majoie, C. B., Vos, F. M., Reneman, L., . . . Schouten-van Meeteren, A. Y. (2009). White matter fractional anisotropy correlates with speed of processing and motor speed in young childhood cancer survivors. *Int J Radiat Oncol Biol Phys, 74*(3), 837-843. doi:10.1016/j.ijrobp.2008.08.060

Barakat, L. P., Li, Y., Hobbie, W. L., Ogle, S. K., Hardie, T., Volpe, E. M., . . . Deatrick, J. A. (2015). Health-related quality of life of adolescent and young adult survivors of childhood brain tumors. *Psychooncology, 24*(7), 804-811. doi:10.1002/pon.3649

Baron, R. M., & Kenny, D. A. (1986). The moderator-mediator variable distinction in social psychological research: Conceptual, strategic, and statistical consideration. *Journal of Personality and Social Psychology, 51*, 1173-1182.

Bassett, D. S., Nelson, B. G., Mueller, B. A., Camchong, J., & Lim, K. O. (2012). Altered resting state complexity in schizophrenia. *Neuroimage, 59*(3), 2196-2207. doi:10.1016/j.neuroimage.2011.10.002

Baum, G. L., Ciric, R., Roalf, D. R., Betzel, R. F., Moore, T. M., Shinohara, R. T., . . . Satterthwaite, T. D. (2017). Modular segregation of structural brain networks supports the development of executive function in youth. *Current Biology, 27*(11), 1561-1572. doi:10.1016/j.cub.2017.04.051

Bereket, A. (2015). Endocrinologic consequences of pediatric posterior foss atumors. *J Clin Res Pediatr Endocrinol, 7*(4), 253-259.

Best, J. R., & Miller, P. H. (2010). A developmental perspective on executive function. *Child Dev, 81*(6), 1641-1660. doi:10.1111/j.1467-8624.2010.01499.x

Bonilha, L., Jensen, J. H., Baker, N., Breedlove, J., Nesland, T., Lin, J. J., . . . Kuzniecky, R. I. (2015). The brain connectome as a personalized biomarker of seizure outcomes after temporal lobectomy. *Neurology, 84*, 1846-1853.

Briere, M. E., Scott, J. G., McNall-Knapp, R. Y., & Adams, R. L. (2008). Cognitive outcome in pediatric brain tumor survivors: delayed attention deficit at long-term follow-up. *Pediatr Blood Cancer, 50*(2), 337-340. doi:10.1002/pbc.21223

Brinkman, T. M., Reddick, W. E., Luxton, J., Glass, J. O., Sabin, N. D., Srivastava, D. K., . . . Krull, K. R. (2012). Cerebral white matter integrity and executive function in adult survivors of childhood medulloblastoma. *Neuro Oncol, 14 Suppl 4*, iv25-iv36. doi:10.1093/neuonc/nos214

Bullmore, E., & Sporns, O. (2009). Complex brain networks: graph theoretical analysis of structural and functional systems. *Nat Rev Neurosci, 10*(3), 186-198. doi:10.1038/nrn2575

Busch, R. M., McBride, A., Curtiss, G., & Vanderploeg, R. D. (2005). The components of executive functioning in traumatic brain injury. *J Clin Exp Neuropsychol, 27*(8), 1022-1032. doi:10.1080/13803390490919263

Butler, R. W., & Copeland, D. R. (2002). Attentional processes and their remediation in chidlren treated for cancer: A literature review and the development of a therapeutic approach. *Journal of the International Neuropsychological Society, 8*, 115-124.

Butler, R. W., Fairclough, D. L., Katz, E. R., Kazak, A. E., Noll, R. B., Thompson, R. D., & Sahler, O. J. (2013). Intellectual functioning and multi-dimensional attentional processes in long-term survivors of a central nervous system related pediatric malignancy. *Life Sci, 93*(17), 611-616. doi:10.1016/j.lfs.2013.05.017

Caeyenberghs, K., Leemans, A., De Decker, C., Heitger, M., Drijkoningen, D., Linden, C. V., . . . Swinnen, S. P. (2012). Brain connectivity and postural control in young traumatic brain injury patients: A diffusion MRI based network analysis. *Neuroimage Clin, 1*(1), 106-115. doi:10.1016/j.nicl.2012.09.011

Caeyenberghs, K., Leemans, A., Leunissen, I., Gooijers, J., Michiels, K., Sunaert, S., & Swinnen, S. P. (2014). Altered structural networks and executive deficits in traumatic brain injury patients. *Brain Struct Funct, 219*(1), 193-209. doi:10.1007/s00429-012-0494-2

Cao, M., Huang, H., & He, Y. (2017). Developmental Connectomics from Infancy through Early Childhood. *Trends Neurosci, 40*(8), 494-506. doi:10.1016/j.tins.2017.06.003

Castellanos, F. X., Di Martino, A., Craddock, R. C., Mehta, A. D., & Milham, M. P. (2013). Clinical applications of the functional connectome. *Neuroimage, 80*, 527-540. doi:10.1016/j.neuroimage.2013.04.083

Chapman, C. A., Waber, D. P., Bernstein, J. H., Pomeroy, S. L., LaVally, B., Sallan, S. E., & Tarbell, N. (1995). Neurobehavioral and neurologic outcome in long-term survivors of posterior fossa brain tumors: role of age and perioperative factors. *J Child Neurol, 10*(3), 209-212.

Chen, Z., Liu, M., Gross, D. W., & Beaulieu, C. (2013). Graph theoretical analysis of developmental patterns of the white matter network. *Front Hum Neurosci, 7*, 716. doi:10.3389/fnhum.2013.00716

Connor, M., Karunamuni, R., McDonald, C., White, N., Pettersson, N., Moiseenko, V., . . . Hattangadi-Gluth, J. (2016). Dose-dependent white matter damage after brain radiotherapy. *Radiother Oncol, 121*(2), 209-216. doi:10.1016/j.radonc.2016.10.003

Crofts, J. J., Higham, D. J., Bosnell, R., Jbabdi, S., Matthews, P. M., Behrens, T. E., & Johansen-Berg, H. (2011). Network analysis detects changes in the contralesional hemisphere following stroke. *Neuroimage, 54*(1), 161-169. doi:10.1016/j.neuroimage.2010.08.032

Crom, D. B., Li, Z., Brinkman, T. M., Hudson, M. M., Armstrong, G. T., Neglia, J., & Ness, K. K. (2014). Life satisfaction in adult survivors of childhood brain tumors. *J Pediatr Oncol Nurs, 31*(6), 317-326. doi:10.1177/1043454214534532

Crossley, N. A., Mechelli, A., Scott, J., Carletti, F., Fox, P. T., McGuire, P., & Bullmore, E. T. (2014a). The hubs of the human connectome are generally implicated in the anatomy of brain disorders. *Brain, 137*(8), 2382-2395. doi:10.1093/brain/awu132

Crossley, N. A., Mechelli, A., Scott, J., Carletti, F., Fox, P. T., McGuire, P., & Bullmore, E. T. (2014b). The hubs of the human connectome are generally implicated in the anatomy of brain disorders. *Brain, 137*(Pt 8), 2382-2395. doi:10.1093/brain/awu132

Cui, Z., Zhong, S., Xu, P., He, Y., & Gong, G. (2013). PANDA: A pipeline toolbox for analyzing brain diffusion images. *Frontiers in Human Neuroscience, 7*(42), 1-16. doi:10.3389/fnhum.2013.00042

de Ruiter, M. A., van Mourik, R., Schouten-van Meeteren, A. Y., Grootenhuis, M. A., & Oosterlaan, J. (2013). Neurocognitive consequences of a paediatric brain tumour and its treatment: a meta-analysis. *Dev Med Child Neurol, 55*(5), 408-417. doi:10.1111/dmcn.12020

Delis, D. C., Kaplan, E., & Kramer, J. H. (2001). *Delis-Kaplan Executive Function System*. San Antonio, TX: The Psychological Corporation.

Drakesmith, M., Caeyenberghs, K., Dutt, A., Lewis, G., David, A. S., & Jones, D. K. (2015). Overcoming the effects of false positives and threshold bias in graph theoretical analyses of neuroimaging data. *Neuroimage, 118*, 313-333. doi:10.1016/j.neuroimage.2015.05.011

Duckworth, J., Nayiager, T., Pullenayegum, E., Whitton, A., hollenberg, R., Horsman, J., . . . Barr, R. D. (2015). Health-realted quality of life in long-term survivors of brain tumors in childhood and adolescence: A serial study spanning a decade. *J Pediatr Hematol Oncol, 37*, 362-367.

Edelstein, K., Spiegler, B. J., Fung, S., Panzarella, T., Mabbott, D. J., Jewitt, N., . . . Hodgson, D. C. (2011). Early aging in adult survivors of childhood medulloblastoma: long-term neurocognitive, functional, and physical outcomes. *Neuro Oncol, 13*(5), 536-545. doi:10.1093/neuonc/nor015

Ehrstedt, C., Kristiansen, I., Ahlsten, G., Casar-Borota, O., Dahl, M., Libard, S., & Stromberg, B. (2016). Clinical characteristics and late effects in CNS tumours of childhood: Do not forget long term follow-up of the low grade tumours. *Eur J Paediatr Neurol, 20*(4), 580-587. doi:10.1016/j.ejpn.2016.04.009

Ellenberg, L., Liu, Q., Gioia, G., Yasui, Y., Packer, R. J., Mertens, A., . . . Zeltzer, L. K. (2009). Neurocognitive status in long-term survivors of childhood CNS malignancies: a report from the Childhood Cancer Survivor Study. *Neuropsychology, 23*(6), 705-717. doi:10.1037/a0016674

Fagerholm, E. D., Hellyer, P. J., Scott, G., Leech, R., & Sharp, D. J. (2015). Disconnection of network hubs and cognitive impairment after traumatic brain injury. *Brain, 138*(Pt 6), 1696-1709. doi:10.1093/brain/awv075

Felicetti, F., D'Ascenzo, F., Moretti, C., Corrias, A., Omede, P., Marra, W. G., . . . Gaita, F. (2015). Prevalence of cardiovascular risk factors in long-term survivors of childhood cancer: 16 years follow up from a prospective registry. *Eur J Prev Cardiol, 22*(6), 762-770. doi:10.1177/2047487314529348

Finc, K., Bonna, K., Lewandowska, M., Wolak, T., Nikadon, J., Dreszer, J., . . . Kuhn, S. (2017). Transition of the functional brain network related to increasing cognitive demands. *Hum Brain Mapp*. doi:10.1002/hbm.23621

First, M. B., Spitzer, R. L., Gibbon, M., & Williams, J. B. W. (1997). *Structured Clinical Interview for DSM-IV axis 1 disorders (SCID-I)-clinical version*. Arlington, VA: American Psychiatric Publishing.

Fischer, F. U., Wolf, D., Scheurich, A., & Fellgiebel, A. (2014). Association of structural global brain network properties with intelligence in normal aging. *PLoS One, 9*(1), e86258. doi:10.1371/journal.pone.0086258

Geenen, M. M., Cardous-Ubbink, M. C., Kremer, L. C., van den Bos, C., Van der Pal, H. J., Heinen, R. C., . . . Van Leeuwen, F. E. (2007). Medical assessment of adverse health outcomes in long-term survivors of childhood cancer. *Journal of American Medical Association, 297*(24), 2705-2715.

Glasser, M. F., Coalson, T. S., Robinson, E. C., Hacker, C. D., Harwell, J., Yacoub, E., . . . Van Essen, D. C. (2016). A multi-modal parcellation of human cerebral cortex. *Nature, 536*(7615), 171-178. doi:10.1038/nature18933

Gragert, M. N., & Ris, M. D. (2011). Neuropsychological late effects and rehabilitation following pediatric brain tumor. *J Pediatr Rehabil Med, 4*(1), 47-58. doi:10.3233/PRM-2011-0153

Greene-Schloesser, D., Moore, E., & Robbins, M. E. (2013). Molecular pathways: radiation-induced cognitive impairment. *Clin Cancer Res, 19*(9), 2294-2300. doi:10.1158/1078-0432.CCR-11-2903

Greene-Schloesser, D., Robbins, M. E., Peiffer, A. M., Shaw, E. G., Wheeler, K. T., & Chan, M. D. (2012). Radiation-induced brain injury: A review. *Front Oncol, 2*, 73. doi:10.3389/fonc.2012.00073

Gunnes, M. W., Lie, R. T., Bjorge, T., Ghaderi, S., Ruud, E., Syse, A., & Moster, D. (2016). Reproduction and marriage among male survivors of cancer in childhood, adolescence and young adulthood: a national cohort study. *Br J Cancer, 114*(3), 348-356. doi:10.1038/bjc.2015.455

Hagmann, P., Cammoun, L., Gigandet, X., Meuli, R., Honey, C. J., Wedeen, V. J., & Sporns, O. (2008). Mapping the structural core of human cerebral cortex. *PLOS Biology, 6*(7), 1479-1493. doi:10.1371/journal.pbio.0050159

Han, K., Mac Donald, C. L., Johnson, A. M., Barnes, Y., Wierzechowski, L., Zonies, D., . . . Brody, D. L. (2014). Disrupted modular organization of resting-state cortical functional connectivity in U.S. military personnel following concussive 'mild' blast-related traumatic brain injury. *Neuroimage, 84*, 76-96. doi:10.1016/j.neuroimage.2013.08.017

Hart, M. G., Ypma, R. J., Romero-Garcia, R., Price, S. J., & Suckling, J. (2016). Graph theory analysis of complex brain networks: new concepts in brain mapping applied to neurosurgery. *J Neurosurg, 124*(6), 1665-1678. doi:10.3171/2015.4.JNS142683

Hayes, A. F. (2009). Beyond Baron and Kenny: Statistical mediation analyses in the new millennium. *Communication Monographs, 76*(4), 408-420. doi:10.1080/03637750903310360

He, Y., & Evans, A. (2010). Graph theoretical modeling of brain connectivity. *Curr Opin Neurol, 23*(4), 341-350. doi:10.1097/WCO.0b013e32833aa567

Hobbie, W. L., Ogle, S. K., Reilly, M., Barakat, L. P., Lucas, M. S., Ginsberg, J. P., . . . Deatrick, J. A. (2016). Adolescent and young adult survivors of childhood brain tumors. *Cancer Nursing, 39*(2), 134-143.

Hocking, M. C., Hobbie, W. L., Deatrick, J. A., Hardie, T. L., & Barakat, L. P. (2015). Family Functioning Mediates the Association Between Neurocognitive Functioning and Health-Related Quality of Life in Young Adult Survivors of Childhood Brain Tumors. *J Adolesc Young Adult Oncol, 4*(1), 18-25. doi:10.1089/jayao.2014.0022

Hollingshead, A. B. (1975). *Four factor index of social status*. Department of Sociology, Yale University. New Haven, CT.

Hummel, Y. M., Hooimeijer, H. L., Zwart, N., Tissing, W. J., Gietema, J. A., Voors, A. A., & van den Berg, M. P. (2015). Long-term cardiac abnormalities after cranial radiotherapy in childhood cancer survivors. *Acta Oncol, 54*(4), 515-521. doi:10.3109/0284186X.2014.969845

Inskip, P. D., Sigurdson, A. J., Veiga, L., Bhatti, P., Ronckers, C., Rajaraman, P., . . . Neglia, J. P. (2016). Radiation-Related New Primary Solid Cancers in the Childhood Cancer Survivor Study: Comparative Radiation Dose Response and Modification of Treatment Effects. *Int J Radiat Oncol Biol Phys, 94*(4), 800-807. doi:10.1016/j.ijrobp.2015.11.046

Jayakar, R., King, T. Z., Morris, R., & Na, S. (2015). Hippocampal volume and auditory attention on a verbal memory task with adult survivors of pediatric brain tumor. *Neuropsychology, 29*(2), 303-319. doi:10.1037/neu0000183

Jbabdi, S., Sotiropoulos, S. N., Haber, S. N., Van Essen, D. C., & Behrens, T. E. (2015). Measuring macroscopic brain connections in vivo. *Nat Neurosci, 18*(11), 1546-1555. doi:10.1038/nn.4134

Jenkinson, M., Bannister, P. R., Brady, J. M., & Smith, S. M. (2002). Improved optimisation for the robust and accurate linear registration and motion correction of brain images. *Neuroimage, 17*(2), 825-841.

Jenkinson, M., Beckmann, C., Behrens, T., Woolrich, M. W., & Smith, S. M. (2012). FSL. *Neuroimage, 62*, 782-790.

Jenkinson, M., & Smith, S. M. (2001). A global optimisation method for robust affine registration of brain images. *Medical Image Analysis, 5*(2), 143-156.

Ji, G. J., Zhang, Z., Xu, Q., Wei, W., Wang, J., Wang, Z., . . . Lu, G. (2015). Connectome Reorganization Associated With Surgical Outcome in Temporal Lobe Epilepsy. *Medicine (Baltimore), 94*(40), e1737. doi:10.1097/MD.0000000000001737

Kelaghan, J., Myers, M. H., Mulvihill, J. J., Byrne, J., COnnelly, R. R., Austin, D. F., . . . Holmes, F. F. (1988). Educational achievement of long-term survivors of childhood and adolescent cancer. *Meidcal and Pediatric Oncology, 16*, 320-326.

Khong, P. L., Kwong, D. L., Chan, G. C., Sham, J. S., Chan, F. L., & Ooi, G. C. (2003). Diffusion-tensor imaging for the detection and quantification of treatment-induced white matter injury in children with medulloblastoma: a pilot study. *AJNR Am J Neuroradiol, 24*(4), 734-740.

Khong, P. L., Leung, L. H., Fung, A. S., Fong, D. Y., Qiu, D., Kwong, D. L., . . . Chan, G. C. (2006). White matter anisotropy in post-treatment childhood cancer survivors:

preliminary evidence of association with neurocognitive function. *J Clin Oncol, 24*(6), 884-890. doi:10.1200/jco.2005.02.4505

Kim, J., Parker, D., Whyte, J., Hart, T., Pluta, J., Ingalhalikar, M., . . . Verma, R. (2014). Disrupted structural connectome is associated with both psychometric and real-world neuropsychological impairment in diffuse traumatic brain injury. *J Int Neuropsychol Soc, 20*(9), 887-896. doi:10.1017/S1355617714000812

King, T. Z., Ailion, A. S., Fox, M. E., & Hufstetler, S. M. (2017). Neurodevelopmental model of long-term outcomes of adult survivors of childhood brain tumors. *Child Neuropsychol*, 1-21. doi:10.1080/09297049.2017.1380178

King, T. Z., & Na, S. (2016). Cumulative neurological factors associated with long-term outcomes in adult survivors of childhood brain tumors. *Child Neuropsychol, 22*(6), 748-760. doi:10.1080/09297049.2015.1049591

King, T. Z., Smith, K. M., & Ivanisevic, M. (2015). The Mediating Role of Visuospatial Planning Skills on Adaptive Function Among Young-Adult Survivors of Childhood Brain Tumor. *Arch Clin Neuropsychol, 30*(5), 394-403. doi:10.1093/arclin/acv033

King, T. Z., Wang, L., & Mao, H. (2015). Disruption of White Matter Integrity in Adult Survivors of Childhood Brain Tumors: Correlates with Long-Term Intellectual Outcomes. *PLoS One, 10*(7), e0131744. doi:10.1371/journal.pone.0131744

Krishnamurthy, S., & Li, J. (2014). New concepts in the pathogenesis of hydrocephalus. *Transl Pediatr, 3*(3), 185-194. doi:10.3978/j.issn.2224-4336.2014.07.02

Lassaletta, A., Bouffet, E., Mabbott, D., & Kulkarni, A. V. (2015). Functional and neuropsychological late outcomes in posterior fossa tumors in children. *Childs Nerv Syst, 31*(10), 1877-1890. doi:10.1007/s00381-015-2829-9

Law, N., Bouffet, E., Laughlin, S., Laperriere, N., Briere, M. E., Strother, D., . . . Mabbott, D. (2011). Cerebello-thalamo-cerebral connections in pediatric brain tumor patients: impact on working memory. *Neuroimage, 56*(4), 2238-2248. doi:10.1016/j.neuroimage.2011.03.065

Lazar, M., Alexander, A. L., Thottakara, P. J., Badie, B., & Field, A. S. (2005). White matter reorganization after surgical resection of brain tumors and vascular malformations. *Am J Neuroradiol, 27*, 1258-1271.

Li, L., Hu, X., Preuss, T. M., Glasser, M. F., Damen, F. W., Qiu, Y., & Rilling, J. (2013). Mapping putative hubs in human, chimpanzee and rhesus macaque connectomes via diffusion tractography. *Neuroimage, 80*, 462-474. doi:10.1016/j.neuroimage.2013.04.024

Li, Y., Liu, Y., Li, J., Qin, W., Li, K., Yu, C., & Jiang, T. (2009). Brain anatomical network and intelligence. *PLOS Computational Biology, 5*(5), e1000395. doi:10.1371/journal.pcbi.1000395

Lin, J. Y., Jackson, I. L., & Vujaskovic, Z. (2016). Mechanisms of Normal Tissue Response. 1-28. doi:10.1007/978-3-319-45594-5_1

Mabbott, D. J., Noseworthy, M., Bouffet, E., Laughlin, S., & Rockel, C. (2006). White matter growth as a mechanism of cognitive development in children. *Neuroimage, 33*(3), 936-946. doi:10.1016/j.neuroimage.2006.07.024

Mabbott, D. J., Noseworthy, M. D., Bouffet, E., Rockel, C., & Laughlin, S. (2006). Diffusion tensor imaging of white matter after cranial radiation in children for medulloblastoma: correlation with IQ. *Neuro Oncol, 8*(3), 244-252. doi:10.1215/15228517-2006-002

Manly, J. J., Byrd, D. A., & Touradji, P. (2004). Acculturation, reading level, and neuropsychological test performance among African American elders. *Applied Neuropsychology, 2004*(11), 1.

Manly, J. J., Jacobs, D. M., Touradji, P., Small, S. A., & Stern, Y. (2002). Reading level attenuates differences in neuropsychological test performance between African American and White elders. *Journal of the International Neuropsychological Society, 8*(03), 341-348. doi:10.1017/s1355617702813157

McClellan, W., Klemp, J. R., Krebill, H., Ryan, R., Nelson, E. L., Panicker, J., . . . Stegenga, K. (2013). Understanding the functional late effects and informational needs of adult survivors of childhood cancer. *Oncol Nurs Forum, 40*(3), 254-262. doi:10.1188/13.ONF.254-262

McCurdy, M. D., Rane, S., Daly, B. P., & Jacobson, L. A. (2016). Associations among treatment-related neurological risk factors and neuropsychological functioning in survivors of childhood brain tumor. *J Neurooncol, 127*(1), 137-144. doi:10.1007/s11060-015-2021-9

McCurdy, M. D., Turner, E. M., Barakat, L. P., Hobbie, W. L., Deatrick, J. A., Paltin, I., . . . Hocking, M. C. (2016). Discrepancies among Measures of Executive Functioning in a Subsample of Young Adult Survivors of Childhood Brain Tumor: Associations with Treatment Intensity. *J Int Neuropsychol Soc, 22*(9), 900-910. doi:10.1017/S1355617716000771

Messe, A., Caplain, S., Pelegrini-Issac, M., Blancho, S., Levy, R., Aghakhani, N., . . . Lehericy, S. (2013). Specific and evolving resting-state network alterations in post-concussion

syndrome following mild traumatic brain injury. *PLoS One, 8*(6), e65470.

doi:10.1371/journal.pone.0065470

Meyer-Base, A., Roberts, R. G., Illan, I. A., Meyer-Base, U., Lobbes, M., Stadlbauer, A., &

Pinker-Domenig, K. (2017). Dynamical Graph Theory Networks Methods for the

Analysis of Sparse Functional Connectivity Networks and for Determining Pinning

Observability in Brain Networks. *Front Comput Neurosci, 11*, 87.

doi:10.3389/fncom.2017.00087

Micklewright, J. L., King, T. Z., Morris, R. D., & Krawiecki, N. (2008). Quantifying pediatric

neuro-oncology risk factors: development of the neurological predictor scale. *J Child

Neurol, 23*(4), 455-458. doi:10.1177/0883073807309241

Moberget, T., Andersson, S., Lundar, T., Due-Tonnessen, B. J., Heldal, A., Endestad, T., &

Westlye, L. T. (2015). Long-term supratentorial brain structure and cognitive function

following cerebellar tumour resections in childhood. *Neuropsychologia, 69*, 218-231.

doi:10.1016/j.neuropsychologia.2015.02.007

Moleski, M. (2000). Neuropsychological, neuroanatomical, and neurophysiological

consequences of CNS chemotherapy for acute lymphoblastic leukemia. *Archives of

Clinical Neuropsychology, 15*(7), 603-630.

Mulhern, R. K., Merchant, T. E., Gajjar, A., Reddick, W. E., & Kun, L. E. (2004). Late

neurocognitive sequelae in survivors of brain tumours in childhood. *Lancet Oncol, 5*(7),

399-408. doi:10.1016/S1470-2045(04)01507-4

Murdaugh, D. L., King, T. Z., & O'Toole, K. (2017). The efficacy of a pilot pediatric cognitive

remediation summer program to prepare for transition of care. *Child Neuropsychology*.

doi:10.1080/09297049.2017.1391949

Nagel, B. J., Palmer, S. L., Reddick, W. E., Glass, J. O., Helton, K. J., Wu, S., . . . Mulhern, R. K. (2004). Abnormal hippocampal development in children with medulloblastoma treated with risk-adapted irradiation. *AJNR Am J Neuroradiol, 25*(9), 1575-1582.

Nayiager, T., Duckworth, J., Pullenayegum, E., Whitton, A., Hollenberg, R., Horsman, J., . . . Barr, R. D. (2015). Exploration of morbidity in a serial study of long-term brain tumor survivors: A focus on pain. *Journal of Adolescent and Young Adult Oncology, 4*(3), 129-136.

Nilsson, D., Rutka, J. T., Snead, O. C., 3rd, Raybaud, C. R., & Widjaja, E. (2008). Preserved structural integrity of white matter adjacent to low-grade tumors. *Childs Nerv Syst, 24*(3), 313-320. doi:10.1007/s00381-007-0466-7

Onoda, K., & Yamaguchi, S. (2015). Dissociative contributions of the anterior cingulate cortex to apathy and depression: Topological evidence from resting-state functional MRI. *Neuropsychologia, 77*, 10-18. doi:10.1016/j.neuropsychologia.2015.07.030

Oouchi, H., Yamada, K., Sakai, K., Kizu, O., Kubota, T., Ito, H., & Nishimura, T. (2007). Diffusion anisotropy measurement of brain white matter is affected by voxel size: underestimation occurs in areas with crossing fibers. *AJNR Am J Neuroradiol, 28*(6), 1102-1106. doi:10.3174/ajnr.A0488

Ostrom, Q. T., Gittleman, H., Xu, J., Kromer, C., Wolinsky, Y., Kruchko, C., & Barnholtz-Sloan, J. S. (2016). CBTRUS statistical report: Primary brain and other central nervous system tumors diagnosed in the United States in 2009-2013. *Neuro Oncol, 18*, v1-v75.

Palmer, S. L., Glass, J. O., Li, Y., Ogg, R., Qaddoumi, I., Armstrong, G. T., . . . Reddick, W. E. (2012). White matter integrity is associated with cognitive processing in patients treated

for a posterior fossa brain tumor. *Neuro Oncol, 14*(9), 1185-1193. doi:10.1093/neuonc/nos154

Panigrahy, A., Schmithorst, V. J., Wisnowski, J. L., Watson, C. G., Bellinger, D. C., Newburger, J. W., & Rivkin, M. J. (2015). Relationship of white matter network topology and cognitive outcome in adolescents with d-transposition of the great arteries. *Neuroimage Clin, 7*, 438-448. doi:10.1016/j.nicl.2015.01.013

Papazoglou, A., King, T. Z., Morris, R. D., & Krawiecki, N. S. (2008). Cognitive predictors of adaptive functioning vary according to pediatric brain tumor location. *Dev Neuropsychol, 33*(4), 505-520. doi:10.1080/87565640802101490

Petrella, J. R. (2011). Use of graph theory to evaluate brain networks: A clinical tool for a small world? *Radiology, 259*, 317-320. doi:10.1148/radiol.11110380

Porter, K. R., McCarthy, B. J., Freels, S., Kim, Y., & Davis, F. G. (2010). Prevalence estimates for primary brain tumors in the United States by age, gender, behavior, and histology. *Neuro Oncol, 12*(6), 520-527. doi:10.1093/neuonc/nop066

Power, J. D., Barnes, K. A., Snyder, A. Z., Schlaggar, B. L., & Petersen, S. E. (2012). Spurious but systematic correlations in functional connectivity MRI networks arise from subject motion. *Neuroimage, 59*(3), 2142-2154. doi:10.1016/j.neuroimage.2011.10.018

Preacher, K. J., & Hayes, A. F. (2004). SPSS and SAS procedures for estimating indirect effects in simple mediation models. *Behavior Research Methods, Instruments, & Computers, 36*(4), 717-731.

Qiu, D., Kwong, D. L., Chan, G. C., Leung, L. H., & Khong, P. L. (2007). Diffusion tensor magnetic resonance imaging finding of discrepant fractional anisotropy between the frontal and parietal lobes after whole-brain irradiation in childhood medulloblastoma

survivors: reflection of regional white matter radiosensitivity? *Int J Radiat Oncol Biol Phys, 69*(3), 846-851. doi:10.1016/j.ijrobp.2007.04.041

Reddick, W. E., Glass, J. O., Palmer, S. L., Wu, S., Gajjar, A., Langston, J. W., . . . Mulhern, R. K. (2005). Atypical white matter volume development in children following craniospinal irradiation. *Neuro Oncol, 7*(1), 12-19. doi:10.1215/S1152851704000079

Reddick, W. E., Taghipour, D. J., Glass, J. O., Ashford, J., Xiong, X., Wu, S., . . . Conklin, H. M. (2014). Prognostic factors that increase the risk for reduced white matter volumes and deficits in attention and learning for survivors of childhood cancers. *Pediatr Blood Cancer, 61*(6), 1074-1079. doi:10.1002/pbc.24947

Reijmer, Y. D., Fotiadis, P., Martinez-Ramirez, S., Salat, D. H., Schultz, A., Shoamanesh, A., . . . Greenberg, S. M. (2015). Structural network alterations and neurological dysfunction in cerebral amyloid angiopathy. *Brain, 138*(Pt 1), 179-188. doi:10.1093/brain/awu316

Ren, X., St Clair, D. K., & Butterfield, D. A. (2017). Dysregulation of cytokine mediated chemotherapy induced cognitive impairment. *Pharmacol Res, 117*, 267-273. doi:10.1016/j.phrs.2017.01.001

Ridley, B. G., Rousseau, C., Wirsich, J., Le Troter, A., Soulier, E., Confort-Gouny, S., . . . Guye, M. (2015). Nodal approach reveals differential impact of lateralized focal epilepsies on hub reorganization. *Neuroimage, 118*, 39-48. doi:10.1016/j.neuroimage.2015.05.096

Riggs, L., Bouffet, E., Laughlin, S., Laperriere, N., Liu, F., Skocic, J., . . . Mabbott, D. J. (2014). Changes to memory structures in children treated for posterior fossa tumors. *J Int Neuropsychol Soc, 20*(2), 168-180. doi:10.1017/S135561771300129X

Ris, M. D., & Beebe, D. W. (2008). Neurodevelopmental outcomes of children with low-grade gliomas. *Dev Disabil Res Rev, 14*(3), 196-202. doi:10.1002/ddrr.27

Ris, M. D., & Noll, R. B. (1994). Long-term neurobehavioral outcome in pediatric brain-tumor

    patients: review and methodological critique. *J Clin Exp Neuropsychol, 16*(1), 21-42.

    doi:10.1080/01688639408402615

Riva, D., Giorgi, C., Nichelli, F., Bulgheroni, S., Massimino, M., Cefalo, G., . . . Pantaleoni, C.

    (2002). Intrathecal methotrexate affects cognitive function in cildren with

    medulloblastoma. *Neurology, 59*(1), 48-53.

Robinson, K. E., Fraley, C. E., Pearson, M. M., Kuttesch, J. F., Jr., & Compas, B. E. (2013).

    Neurocognitive late effects of pediatric brain tumors of the posterior fossa: a quantitative

    review. *J Int Neuropsychol Soc, 19*(1), 44-53. doi:10.1017/s1355617712000987

Robinson, K. E., Kuttesch, J. F., Champion, J. E., Andreotti, C. F., Hipp, D. W., Bettis, A., . . .

    Compas, B. E. (2010). A quantitative meta-analysis of neurocognitive sequelae in

    survivors of pediatric brain tumors. *Pediatr Blood Cancer, 55*(3), 525-531.

    doi:10.1002/pbc.22568

Robison, L. L., Green, D. M., Hudson, M., Meadows, A. T., Mertens, A. C., Packer, R. J., . . .

    Zeltzer, L. K. (2005). Long-term outcomes of adult survivors of childhood cancer.

    Cancer, 104(11 Suppl), 2557-2564. doi:10.1002/cncr.21249

Rubinov, M., & Sporns, O. (2010). Complex network measures of brain connectivity: uses and

    interpretations. *Neuroimage, 52*(3), 1059-1069. doi:10.1016/j.neuroimage.2009.10.003

Rueckriegel, S. M., Bruhn, H., Thomale, U. W., & Hernaiz Driever, P. (2015). Cerebral white

    matter fractional anisotropy and tract volume as measured by MR imaging are associated

    with impaired cognitive and motor function in pediatric posterior fossa tumor survivors.

    Pediatr Blood Cancer, 62(7), 1252-1258. doi:10.1002/pbc.25485

Rueckriegel, S. M., Driever, P. H., Blankenburg, F., Ludemann, L., Henze, G., & Bruhn, H. (2010). Differences in supratentorial damage of white matter in pediatric survivors of posterior fossa tumors with and without adjuvant treatment as detected by magnetic resonance diffusion tensor imaging. *Int J Radiat Oncol Biol Phys, 76*(3), 859-866. doi:10.1016/j.ijrobp.2009.02.054

Santarnecchi, E., Galli, G., Polizzotto, N. R., Rossi, A., & Rossi, S. (2014). Efficiency of weak brain connections support general cognitive functioning. *Hum Brain Mapp, 35*(9), 4566-4582. doi:10.1002/hbm.22495

Saury, J. M., & Emanuelson, I. (2011). Cognitive consequences of the treatment of medulloblastoma among children. *Pediatr Neurol, 44*(1), 21-30. doi:10.1016/j.pediatrneurol.2010.07.004

Savla, G. N., Twamley, E. W., Delis, D. C., Roesch, S. C., Jeste, D. V., & Palmer, B. W. (2012). Dimensions of executive functioning in schizophrenia and their relationship with processing speed. *Schizophr Bull, 38*(4), 760-768. doi:10.1093/schbul/sbq149

Seaver, E., Geyer, R., Sulzbacher, S., Warner, M., Batzel, L., Milstein, J., & Berger, M. (1994). Psychosocial adjustment in long-term survivors of childhood medulloblastoma and ependymoma treated with craniospinal irradiation. *Pediatr Neurosurg, 20*, 248-253.

Shah, S. S., Dellarole, A., Peterson, E. C., Bregy, A., Komotar, R., Harvey, P. D., & Elhammady, M. S. (2015). Long-term psychiatric outcomes in pediatric brain tumor survivors. *Childs Nerv Syst, 31*(5), 653-663. doi:10.1007/s00381-015-2669-7

Smith, K., King, T. Z., Jayakar, R., & Morris, R. D. (2014). Reading skill in adult survivors of childhood brain tumor: a theory-based neurocognitive model. *Neuropsychology, 28*(3), 448-458. doi:10.1037/neu0000056

Smith, S. M. (2002). Fast robust automated brain extraction. *Human Brain Mapping, 17*(3), 143-155.

Smith, S. M., Jenkinson, M., Woolrich, M. W., Beckmann, C., Behrens, T., Johansen-Berg, H., . . . Matthews, P. M. (2004). Advances in functional and structural MR image analysis and implementation as FSL. *NeuroImage, 23*, 208-219.

Smoll, N. R. (2012). Relative survival of childhood and adult medulloblastomas and primitive neuroectodermal tumors (PNETs). *Cancer, 118*(5), 1313-1322. doi:10.1002/cncr.26387

Spiegler, B. J., Bouffet, E., Greenberg, M. L., Rutka, J. T., & Mabbott, D. J. (2004). Change in neurocognitive functioning after treatment with cranial radiation in childhood. *J Clin Oncol, 22*(4), 706-713. doi:10.1200/JCO.2004.05.186

Sporns, O. (2012). From simple graphs to the connectome: networks in neuroimaging. *Neuroimage, 62*(2), 881-886. doi:10.1016/j.neuroimage.2011.08.085

Stam, C. J., Hillebrand, A., Wang, H., & Van Mieghem, P. (2010). Emergence of Modular Structure in a Large-Scale Brain Network with Interactions between Dynamics and Connectivity. *Front Comput Neurosci, 4*. doi:10.3389/fncom.2010.00133

Stevens, A. A., Tappon, S. C., Garg, A., & Fair, D. A. (2012). Functional brain network modularity captures inter- and intra-individual variation in working memory capacity. *PLoS One, 7*(1), e30468. doi:10.1371/journal.pone.0030468

Stuss, D. T., & Alexander, M. P. (2000). Executive functions and the frontal lobes: a conceptual view. *Psychological Research, 63*, 289-298.

Taiwo, Z., Na, S., & King, T. Z. (2017). The Neurological Predictor Scale: A predictive tool for long-term core cognitive outcomes in survivors of childhood brain tumors. *Pediatr Blood Cancer, 64*(1), 172-179. doi:10.1002/pbc.26203

Tang, J., Zhong, S., Chen, Y., Chen, K., Zhang, J., Gong, G., . . . Zhang, Z. (2015). Aberrant white matter networks mediate cognitive impairment in patients with silent lacunar infarcts in basal ganglia territory. *J Cereb Blood Flow Metab, 35*(9), 1426-1434. doi:10.1038/jcbfm.2015.67

Termenon, M., Achard, S., Jaillard, A., & Delon-Martin, C. (2016). The "Hub Disruption Index," a Reliable Index Sensitive to the Brain Networks Reorganization. A Study of the Contralesional Hemisphere in Stroke. *Front Comput Neurosci, 10*, 84. doi:10.3389/fncom.2016.00084

Testa, R., Bennett, P., & Ponsford, J. (2012). Factor analysis of nineteen executive function tests in a healthy adult population. *Arch Clin Neuropsychol, 27*(2), 213-224. doi:10.1093/arclin/acr112

Turner, C. D., Rey-Casserly, C., Liptak, C., & Chordas, C. (2009). Late effects of therapy for pedatric brain tumor survivors. *J Child Neurol, 24*(11), 1455-1463.

Tzourio-Mazoyer, N., Landeau, B., Papathanassiou, D., Crivello, F., Etard, O., Delcroix, N., . . . Joliot, M. (2002). Automated anatomical labeling of activations in SPM using a macroscopic anatomical parcellation of the MNI MRI single-subject brain. *NeuroImage, 15*, 273-289.

Ullrich, N. J., & Embry, L. (2012). Neurocognitive dysfunction in survivors of childhood brain tumors. *Semin Pediatr Neurol, 19*(1), 35-42. doi:10.1016/j.spen.2012.02.014

van den Heuvel, M. P., & Sporns, O. (2011). Rich-club organization of the human connectome. *J Neurosci, 31*(44), 15775-15786. doi:10.1523/JNEUROSCI.3539-11.2011

van den Heuvel, M. P., & Sporns, O. (2013). Network hubs in the human brain. *Trends Cogn Sci, 17*(12), 683-696. doi:10.1016/j.tics.2013.09.012

van den Heuvel, M. P., Stam, C. J., Kahn, R. S., & Hulshoff Pol, H. E. (2009). Efficiency of functional brain networks and intellectual performance. *J Neurosci, 29*(23), 7619-7624. doi:10.1523/JNEUROSCI.1443-09.2009

van Dijk, I. W., Cardous-Ubbink, M. C., van der Pal, H. J., Heinen, R. C., van Leeuwen, F. E., Oldenburger, F., . . . Kremer, L. C. (2013). Dose-effect relationships for adverse events after cranial radiation therapy in long-term childhood cancer survivors. *Int J Radiat Oncol Biol Phys, 85*(3), 768-775. doi:10.1016/j.ijrobp.2012.07.008

van Straaten, E. C., & Stam, C. J. (2013). Structure out of chaos: functional brain network analysis with EEG, MEG, and functional MRI. *Eur Neuropsychopharmacol, 23*(1), 7-18. doi:10.1016/j.euroneuro.2012.10.010

van Wijk, B. C., Stam, C. J., & Daffertshofer, A. (2010). Comparing brain networks of different size and connectivity density using graph theory. *PLoS One, 5*(10), e13701. doi:10.1371/journal.pone.0013701

Wakana, S., Caprihan, A., Panzenboeck, M. M., Fallon, J. H., Perry, M., Gollub, R. L., . . . Mori, S. (2007). Reproducibility of quantitative tractography methods applied to cerebral white matter. *Neuroimage, 36*(3), 630-644. doi:10.1016/j.neuroimage.2007.02.049

Wang, R., Benner, T., Sorensen, A. G., & Wedeen, V. J. (2007). *Diffusion toolkit: A software package for diffusion imaging data processing and tractography*. Paper presented at the Proc. Intl. Soc. Mag. Reson. Med.

Wechsler, D. (1999). *Wechsler Abbreviated Scale of Intelligence manual*. San Antonio, TX: Harcourt Assessment.

Wei, C. W., Guo, G., & Mikulis, D. J. (2014). Tumor Effects on Cerebral White Matter as Characterized by Diffusion Tensor Tractography. *The Canadian Journal of Neurological Sciences, 34*(01), 62-68. doi:10.1017/s0317167100005801

Wen, W., He, Y., & Sachdev, P. (2011). Structural brain networks and neuropsychiatric disorders. *Curr Opin Psychiatry, 24*(3), 219-225. doi:10.1097/YCO.0b013e32834591f8

Willard, V. W., Klosky, J. L., Li, C., Srivastava, D. K., Brinkman, T. M., Robison, L. L., . . . Phipps, S. (2017). The impact of childhood cancer: Perceptions of adult survivors. *Cancer*. doi:10.1002/cncr.30514

Wolfe, K. R., Madan-Swain, A., & Kana, R. K. (2012). Executive dysfunction in pediatric posterior fossa tumor survivors: a systematic literature review of neurocognitive deficits and interventions. *Dev Neuropsychol, 37*(2), 153-175. doi:10.1080/87565641.2011.632462

Wolfe, K. R., Walsh, K. S., Reynolds, N. C., Mitchell, F., Reddy, A. T., Paltin, I., & Madan-Swain, A. (2013). Executive functions and social skills in survivors of pediatric brain tumor. *Child Neuropsychol, 19*(4), 370-384. doi:10.1080/09297049.2012.669470

Woolrich, M. W., Jbabdi, S., Patenaude, B., Chappell, M., Makni, S., Behrens, T., . . . Smith, S. M. (2009). Bayesian analysis of neuroimaging data in FSL. *NeuroImage, 45*, 173-186.

Yendiki, A., Koldewyn, K., Kakunoori, S., Kanwisher, N., & Fischl, B. (2014). Spurious group differences due to head motion in a diffusion MRI study. *Neuroimage, 88*, 79-90. doi:10.1016/j.neuroimage.2013.11.027

Yuan, W., Wade, S. L., & Babcock, L. (2015). Structural connectivity abnormality in children with acute mild traumatic brain injury using graph theoretical analysis. *Hum Brain Mapp, 36*(2), 779-792. doi:10.1002/hbm.22664

Zhang, L., Yang, H., & Tian, Y. (2015). Radiation-induced cognitive impairment. *Therapeutic Targets for Neurological Diseases, 2*, 1-8. doi:10.14800/ttnd.837

APPENDIX
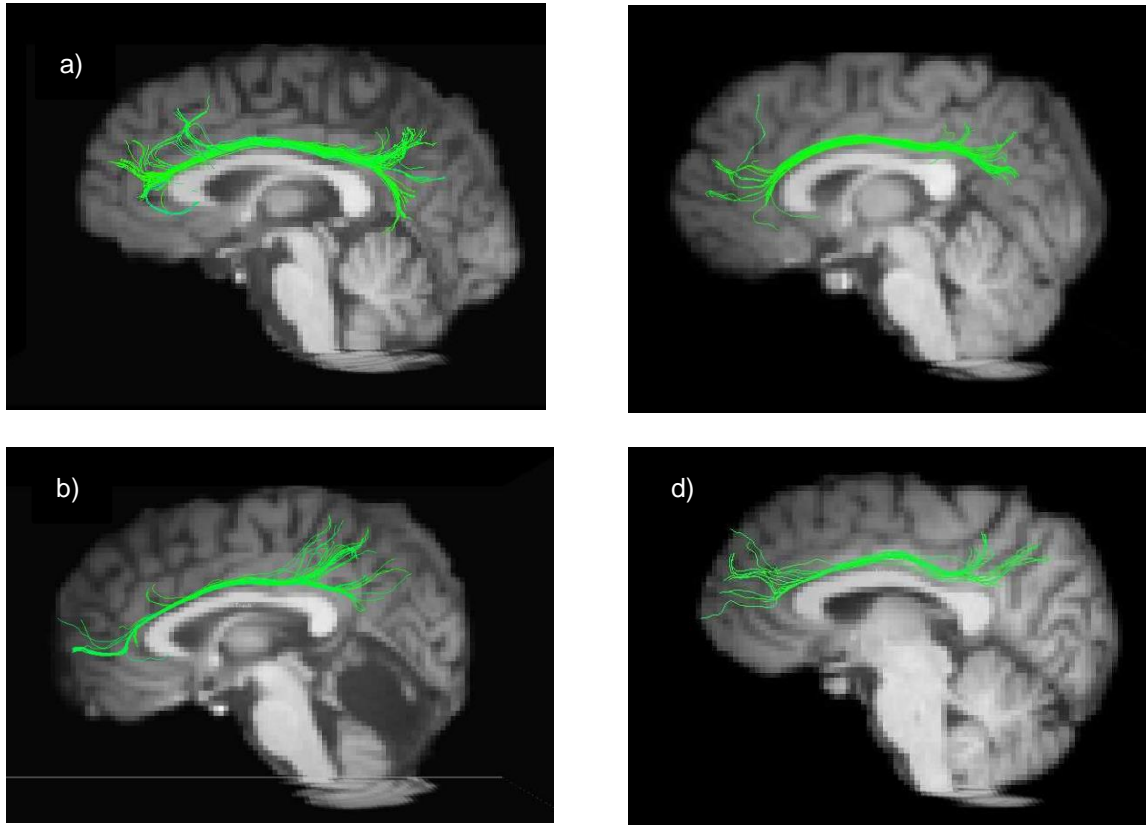
Cingulum in the cingulate gyrus part for two survivors (a and b) and two controls (c and d)